




Journées du GDR NanoTeraMIR

June 9-10, 2021

 Metz (France) – Virtual conference



Book of abstracts

Committees

Bureau of the GDR NanoTeraMIR

- Juliette Mangeney | ENS
- Jean-Louis Coutaz | Université de Savoie
- Georges Humbert | XLIM
- Alexandre Delga | 3-5 Lab
- Sukhdeep Dhillon | ENS
- Delphine Marris-Morini | Université Paris-Sud
- Patrick Mounaix | Université de Bordeaux
- Gaël Mouret | Université du Littoral Côte d'Opale
- Gérard-Pascal Piau | Airbus
- Frédéric Teppe | Université de Montpellier
- Roland Teissier | Université de Montpellier
- Pascale Roy | Synchrotron SOLEIL
- Carlo Sirtori | ENS
- Jean-Francois Lampin | Université de Lille
- Jean Michel Chauveau | Université de Versailles Saint-Quentin-en-Yvelines
- David Citrin | Georgia Institute of Technology
- Alexandre Locquet | IRL 2958 Georgia Tech-CNRS

Organizing committee

- David Citrin | Georgia Institute of Technology
- Alexandre Locquet | IRL 2958 Georgia Tech-CNRS
- Jaume Calvo de la Rosa | Universitat de Barcelona

Table of contents

| | |
|--|----|
| Absorption modulation with semiconductor plasmonic microstructures from 1.1 to 2.5 THz, Gonzalez-Posada Flores Fernando [et al.] | 1 |
| H ₂ S photoacoustic detection with an integrated THz gas sensor for food quality control, Akiki Elias [et al.] | 3 |
| Long-pathlength spectroscopy in Atmospheric Simulation Chamber, from near-infrared to terahertz., Decker Jean [et al.] | 5 |
| Study of Functional Metal Oxides Thin Films using Infrared Synchrotron Radiation, Cervasio Rebecca [et al.] | 7 |
| Non-destructive evaluation of ceramic porosity using terahertz time-domain spectroscopy, Hakobyan Davit [et al.] | 8 |
| MIR and THz Spectroscopy with 10 nm spatial resolution, Schäfer Philip [et al.] | 9 |
| Multimodal vibrational infrared spectroscopy from 1.1 to 6.5 μm with Aluminum Bowties, Najem Melissa [et al.] | 10 |
| Thermal radiation of a single pair of subwavelength antennas, Abou Hamdan Loubnan [et al.] | 11 |
| Cd _{1-y} Zn _y Te ternary alloys: from thermodynamic computations to stoichiometric growth conditions, Modni Sara | 12 |
| Large HgTe nanocrystals for THz technology, Apretna Thibault [et al.] | 13 |

| | |
|--|----|
| VERTICAL MULTILAYER STRUCTURES BASED ON POROUS SILICON LAYERS FOR MID-INFRARED APPLICATIONS, Meziani Sofiane [et al.] | 14 |
| Quantum cascade detectors operating in the strong light-matter coupling regime., Lagrée Mathurin [et al.] | 15 |
| Coating Thickness Mapping Extraction by Time-Domain Terahertz Spectroscopy, Cassar Quentin [et al.] | 16 |
| Terahertz refractive index-based morphological dilation: A strategy towards improving breast conserving surgery, Cassar Quentin [et al.] | 18 |
| THz acquisition and rendering with augmented reality, Guillet Jean-Paul [et al.] | 20 |
| Thz imaging of injection-mold weld lines in ABS thermoplastic, Zhai Min [et al.] | 21 |
| Accounting for the pellet's porosity in THz-TDS measurements of powder oxides, Locquet Alexandre [et al.] | 22 |
| Electroluminescence from HgTe quantum dots and its Use for Active Imaging, Lhuillier Emmanuel [et al.] | 24 |
| Gate tunable colloidal nanocrystal-based infrared sensor, Dang Huu Tung [et al.] | 25 |
| Highly sensitive heterodyne detection with stabilized QCL laser, Saemian Mohammadreza [et al.] | 26 |
| Hot Carrier Semiconductor Plasmonic Mid-infrared Photodetector, Haky Andrew [et al.] | 27 |
| Mid-infrared frequency comb for QCL stabilisation and detectors assessment at $9\mu\text{m}$, Gacemi Djamal [et al.] | 28 |
| Optimizing patch antenna arrays for MIR quantum detectors, Rodriguez Eti- | |

| | |
|---|----|
| enne [et al.] | 29 |
| Room temperature, high speed, mid-infrared Stark-shift modulator on InP, Bonazzi Thomas [et al.] | 31 |
| Strong Anti-correlation in a Quantum Cascade Laser Frequency Comb, Chomet Baptiste [et al.] | 32 |
| High bitrate Free-Space Optical communication at 9 μm wavelength using Unipolar Devices operating at room-temperature, Dely Hamza [et al.] | 33 |
| 280-GHz Radiation Source Driven by a 1064-nm Dual-Frequency Laser, Abbas Alaeddine [et al.] | 35 |
| Low Optical Power-Driven THz Modulator, Guise Julien [et al.] | 36 |
| Polarization control of emitted THz waves using spintronic emitters with anisotropic magnetic layers & birefringence characterization of Quartz, Lezier Geoffrey [et al.] | 37 |
| Magneto-electric control of polarization in spintronic terahertz emitters, Tiercelin Nicolas [et al.] | 38 |
| Terahertz optomechanical resonators with bi-material structures, Liu Jiawen [et al.] | 39 |
| Design and characterisation of Photoswitches for picosecond electric pulses generation at very low temperature, Bernerd Cyril [et al.] | 41 |
| Photon-assisted tunneling in hBN encapsulated graphene quantum dot under coherent THz illumination, Messelot Simon [et al.] | 42 |
| ON-CHIP TWO-OCTAVES SUPERCONTINUUM GENERATION IN MID-IR SIGE WAVEGUIDES, Koompai Natnicha [et al.] | 43 |
| Sub wavelength resonator coupled to colloidal nanocrystal array for short wave infrared sensing with near unity absorption, Chu Audrey [et al.] | 45 |

Absorption modulation with semiconductor plasmonic microstructures from 1.1 to 2.5 THz

F. Gonzalez-Posada[§], D.Coquillat[@], M. Najem[§], P.Loren[§], T. Taliercio[§]

[§]IES, Univ Montpellier, CNRS, Montpellier, France

[@]L2C, Univ Montpellier, CNRS, Montpellier, France

Corresponding author: fernando.gonzalez-posada-flores@umontpellier.fr

Terahertz time domain spectroscopy (THz-TDS) remains so far the backbone of terahertz photonics in numerous applications. [1] Plasmonic microstructures and metasurfaces are particularly promising for improving THz spectroscopy techniques and promising for the development of biomedical and environmental sensors. [2] Highly doped semiconductors are suitable for replacing the traditionally-used noble metals, because their plasmonic behaviors are optically tuned with different geometry, size and interactions (gap effect) also in this spectral range. In figure 1A, a perfect absorber structure based on III-V semiconductor layers is presented on a GaSb commercial substrate template. A photonic absorption peak was targeted in the IR with the thickness of the GaSb spacer on top of a metallic mirror-like doped InAsSb layer. The InAsSb top layer was doped and microstructured to obtain a plasmonic resonance in the THz region. Figure 1B shows the visible light diffraction of the $1 \times 1 \text{ mm}^2$ micro-structure arrays fabricated by electron beam lithography and dry etching. In figure 1C, the darkest $1 \times 1 \text{ mm}^2$ squares correspond to an array of InAsSb linewidth of 14 and 16 μm with a constant pitch of 30 μm . Such contrast is related to the coupling between the plasmonic microstructure array and the incident light at a mean frequency region selected in the THz-TDS measurement. Thus, an intense color indicates a higher electric field in the C-slice view scale. In this particular C-slice view, a 2-2.05 THz mean frequency is selected. Finally, in figure 1D, the THz-TDS measurements of the minimum absorption reached (red dots) correspond with the simulation absorption map calculated by rigorous-coupled wave analysis [3].

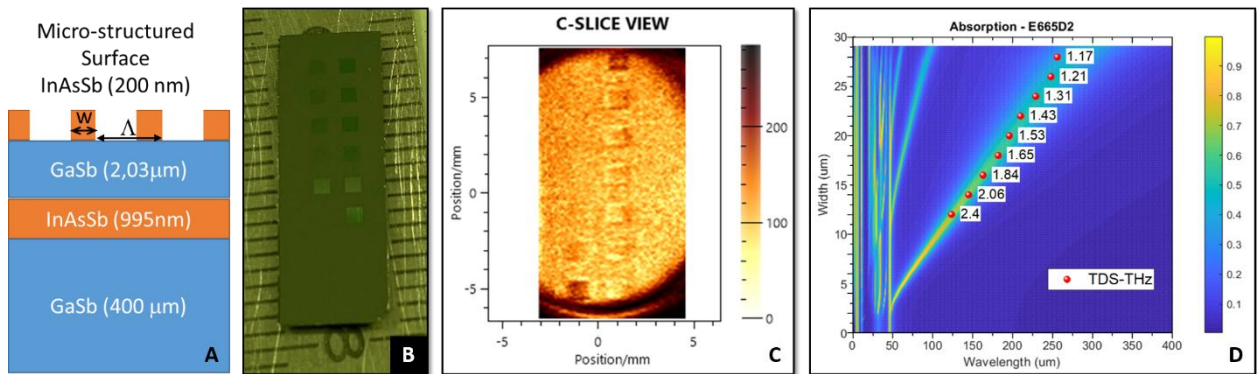


Fig. 1:A) Epitaxial layers from the substrate to the micro-structured surface of InAsSb B) Photograph of the complete transducer sensor with $1 \times 1 \text{ mm}^2$ micro-structured areas with a constant pitch (Λ) of 30 μm and variable linewidth (w) from 2 to 28 μm . C) Electrical field of the transducer surface imaged at 2-2.05 THz frequency. D) Simulation of the absorption of the micro-structured surface for different linewidths corresponding to the electromagnetic THz spectral range (Color map). Absorption minimum mean value of six points for each square measured in the THz-TDS experiments. (Red dots and labels)

References:

- [1] M. Beard et al. J. of Phys. Chem. B 106, 12345 (2002).
- [2] D. M. Mittleman Nature Photonics 7, 666 (2013)
- [3] J.-P. Hugonin, & Lalanne. [Light-in-complex-nanostructures](#) RETICOLO V8 (2020).

Acknowledgements:

This work is partially supported by:

- Equipex EXTRA (ANR-11-EQPX-0016)
- SEA – Region Occitanie (2020-2021)
- MUSE – PRIME@MUSE – I-Site

H₂S photoacoustic detection with an integrated THz gas sensor for food quality control

Elias Akiki[@], Marie-Hélène Mammez[§], Guillaume Ducournau[@], Marc Faucher[@], Benjamin Walter^{*}, Gaël Mouret[§], Jean-François Lampin[@], Mathias Vanwolleghem[@]

[@]Institut d'Electronique de Microélectronique et de Nanotechnologie, UMR CNRS 8520, Villeneuve d'Ascq, France

[§]Laboratoire de Physico-Chimie de l'Atmosphère, Université du Littoral Côte d'Opale, France

^{*}Vmicro SAS, Villeneuve d'Ascq, France

Corresponding author: elias.akiki@univ-lille.fr

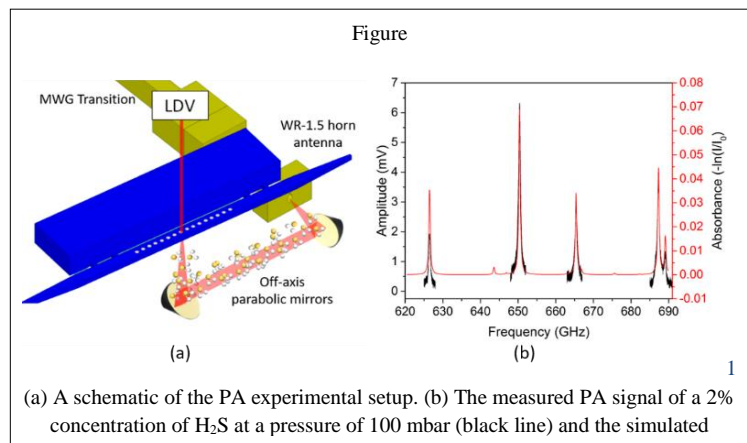
H₂S gas is a toxic molecule emitted by the bacterial growth in food and as such is a great indicator of food spoilage. Monitoring its concentrations to control food quality has been the subject of much research [1], [2]. For instance, in fresh beef meat conserved at 25 °C for 48 hours, the H₂S concentration evolves from 480 ppb to 7.16 ppm [2]. The detection of small H₂S concentrations at sub-ppm levels is necessary to ensure the safety of food consumption. In addition to being an excellent food spoilage indicator, the H₂S gas molecule presents high-intensity absorption peaks in the THz region. THz photoacoustic spectroscopy is a great tool for the detection of such molecules. In [3] we proposed the design of an integrated THz PA gas sensor for monitoring food spoilage. It is based on the confinement of the THz light in a PhC cavity with high Q factors [4] to increase the light-molecules interaction. Gas molecules absorbing the THz modulated light produce sound waves that are enhanced inside an acoustical cylinder which is at the same time the etched hole of the PhC THz cavity and then detected by a Poly-Si microphone covering the bottom of the cylinder. Here we present the detection of H₂S molecules by focusing the THz beam on the Poly-Si membrane and without considering the enhancement inside the THz cavity. A schematic of the experimental setup is presented in figure 1(a). A VDI

electronic source is used to generate a THz signal in the 620-690 GHz frequency range with a power varying between 0.4 and 1.1 mW at the horn antenna output. The amplitude of the THz signal is modulated at the mechanical resonance frequency of the membrane (36.5 kHz) with a 100% duty cycle. A laser Doppler vibrometer (MSA-500 Polytec) is used to detect the mechanical displacement of the Poly-Si membrane. The THz emission frequency is controlled and swept using a Labview interface, collecting the LDV

data through a lock-in amplifier. Figure 1(b) shows a great agreement between the measured and simulated absorption lines for an H₂S gas concentration of 2% at a pressure of 100 mbar. The PA signal is measured with a 16 ms of lock-in integration time while the THz source emission frequency is swept around 5 different absorption peaks of the H₂S. The simulated spectrum was obtained from Spectraplot based on the HITRAN database by using the same experimental parameters and a 10 cm long gas cell. The minimum detection limit (MDL) describes the sensitivity of the sensor and is defined as the lowest detected concentration with an SNR=1. We observe a MDL of 100 ppm of H₂S at 10 mbar. Higher sensitivity with an MDL of 10's of ppb is expected by coupling the poly-Si membrane to the PhC THz high Q cavity (Q =10000 [4]). This is a first step towards a fully integrated THz PA gas sensor with a sensitivity in the order of 10's ppb.

References:

- [1] F. Hindle et al. "Monitoring of food spoilage by high resolution THz analysis", *Analyst* 143, 5536–5544 (2018)
- [2] M. O. Hanna, et al. "Effect of Growth of Individual Meat Bacteria on pH, Color and Odor of Aseptically Prepared Vacuum-Packaged Round Steaks," *J. Food Prot.*, vol. 46, no. 3, pp. 216–221, Mar. 1983
- [3] M. Verstuyft et al., "Proposal for an integrated silicon-photonics terahertz gas detector using photoacoustics," *Opt. Express*, vol. 28, no. 15, pp. 22424–22442, Jul. 2020
- [4] E. Akiki et al., "High Q THz photonic crystal cavity on a low loss suspended Silicon platform," *IEEE Trans. Terahertz Sci. Technol.*, pp. 1– 1, 2020



(a) A schematic of the PA experimental setup. (b) The measured PA signal of a 2% concentration of H₂S at a pressure of 100 mbar (black line) and the simulated

[5]“SpectraPlot.com – Absorption spectroscopy simulator.” <https://www.spectraplot.com/absorption>

Long-pathlength spectroscopy in Atmospheric Simulation Chamber, from near-infrared to terahertz.

Jean Decker, Eric Fertein, Pierre Kulinski, Nicolas Houzel, Jonas Bruckhuisen, Frank Hindle, Gaël Mouret, Robin Bocquet, Guillaume Dhont, Cécile Cœur and Arnaud Cuisset

Laboratoire de Physico-Chimie de l'Atmosphère, UR 4493, LPCA, Université du Littoral Côte d'Opale, F-59140 Dunkerque, France

Corresponding author: jean.decker@univ-littoral.fr

Volatile organic compounds (VOCs) are emitted into the atmosphere by natural processes (vegetation, oceans, etc.) or as a result of human activities (transport, industry, etc.). To study their atmospheric evolution, research work on their reactivity with the main oxidants is carried out into atmospheric simulation chambers (ASC). A new ASC, CHARME for "CHamber for the Atmospheric Reactivity and the Metrology of the Environment", has therefore been developed at the LPCA, in the regional research and technological innovation platform called IReNE ^[1]. The originality of CHARME is its combination with innovative detection methods using optical and electronic sources from the UV-Visible to the TeraHertz (THz) frequency range for in situ and time-resolved monitoring of stable and unstable gas phase molecules involved in atmospheric reactivity processes.

The development of a multi-pass "Chernin type" cell operational from the near-IR to THz/submillimeter wavelengths and its coupling to CHARME with pathlengths adjusted from 120 m. (24 paths) to 280 m. (56 paths) in THz and 480 m (96 paths) in Near-IR allowed to detect and quantify greenhouse gases at trace levels by probing their rotational and rovibrational transitions. While different UV/IR spectrometer equipped the ASC, we are the first to couple a THz source to a ASC and to reach a so long THz path with a multi-pass cell ^[2]. Significant absorbances of 400 ppm residual N₂O traces at 577.58 GHz and 200 ppm O₃ traces have been measured with a path-length adjusted to 200 meters. Right now, the accessible detection levels for both compounds are limited to tens of ppm due to strong variations caused by multiple interfering stationary waves in the Chernin cell. The modelisation of these baseline variations is under progress.

The use of THz spectroscopy in an ASC such CHARME opens new possibilities especially for the monitoring of stratospheric reaction processes at low-pressure or for new measurements of the water vapor continuum at submillimeter wavelengths. Moreover, the versatility of the submillimeter electronic sources will allow to perform time-resolved quantitative spectroscopies of reactants, oxidants and products involved in targeted reactions occurring in the high altitude atmospheric layers.

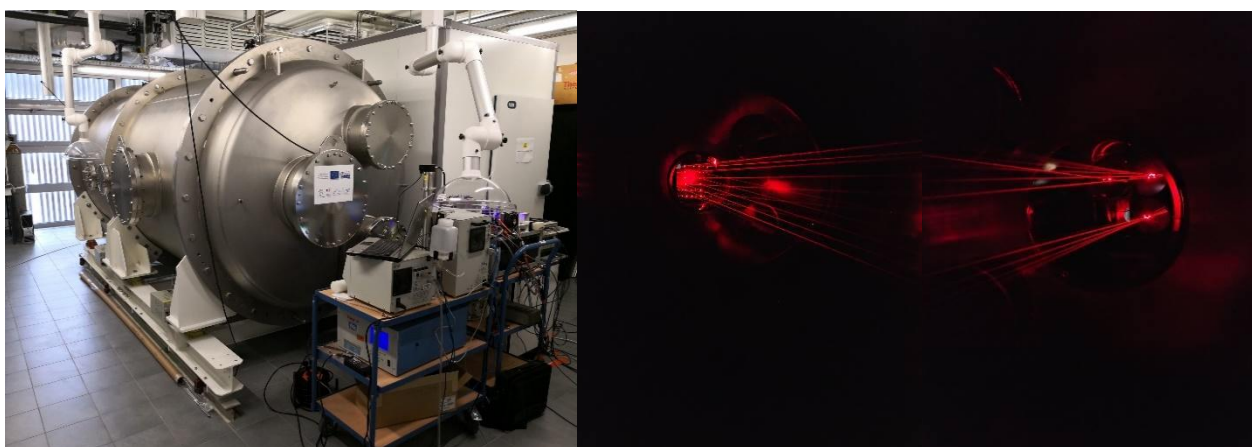


Fig. : left :CHARME right : Chernin multipass cell

References:

[1] Meng, L. et al : Secondary organic aerosol formation from the gas-phase reaction of guaiacol (2-methoxyphenol) with NO₃ radicals. *J.Atmos.408Env.*2020,240, 1117740.

[2] Cuisset, A. et al : Terahertz rotational spectroscopy of greenhouse gases using long interaction path-lengths. *Appl.Sci.*2021,11(3),1229;

Study of Functional Metal Oxides Thin Films using Infrared Synchrotron Radiation

Rebecca CERVASIO, Marine VERSEILS, Jean-Blaise BRUBACH, Pascale ROY

AILES Beamline, Synchrotron SOLEIL

Corresponding author: rebecca.cervasio@synchrotron-soleil.fr

New device applications in materials sciences call for the merging of known physical properties with the nanoscale world. Examples include new ferroelectric materials obtained in thin films of just a few nanometers. These materials are often functional metal oxides, that are present in different technologies such as memory storage, energy harvesting and sensors¹.

However, the spectroscopic study of such functional thin films comes with new challenges. It is important to understand the influence of the film thickness, the substrate, and the interfaces present. All these parameters have a role in the new physical phenomena probed. To control the desired properties, it is necessary to understand the electric and structural signatures responsible for such properties. Exploiting the high brilliance and the stability of the synchrotron radiation in a wide infrared spectral range available at the AILES beamline of SOLEIL, we were able to perform infrared and Terahertz spectroscopic measurements on several thin film materials promising for applications.

One of these materials is the recently discovered HfZrO₂ ferroelectric thin (below 20 nm) film². This unexpected ferroelectricity in such nanometric films has stimulated new research into understanding its origin and opened a path to ferroelectrics memristors³. Beyond these promising applications, many fundamental aspects related to the ferroelectricity order in HfO₂-based systems remain to be unveiled⁴ e.g. ferroelectric transition temperature, role of non-polar coexisting phases, imposed electrode boundary conditions, electrical cycling effects. We report the results obtained from temperature and electric field dependence of transmission infrared and THz spectroscopy measurements.

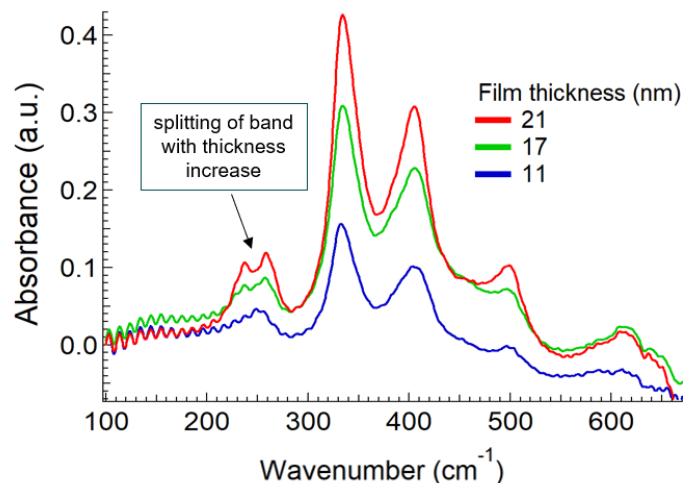


Fig. 1: Far-infrared absorption spectra of three different HfZrO₂ film thickness: 11, 17 and 21 nm. The spectra are in accordance with theoretical calculations of the polar-orthorhombic ferroelectric phase.

References:

1. Setter, N. *et al. Journal of Applied Physics* **100**, 051606 (2006).
2. Chernikova, A. *et al. ACS Appl. Mater. Interfaces* **8**, 7232–7237 (2016).
3. Materlik, R., Künneth, C. & Kersch, A. *Journal of Applied Physics* **117**, 134109 (2015).
4. Shimizu, T. *J. Ceram. Soc. Japan* **126**, 667–674 (2018).

Non-destructive evaluation of ceramic porosity using terahertz time-domain spectroscopy

Davit Hakobyan¹, Maher Hamdi¹, Olivier Redon¹, Anthony Ballestero², Alexis Mayaudon², Laurence Boyer², Olivier Durand², Emmanuel Abraham³

¹ CEA Tech Nouvelle Aquitaine, Coeur Bersol Bâtiment B, 28 Avenue Gustave Eiffel, 33600 Pessac, France

² Center for Technology Transfers in Ceramics, Parc Ester Technopole, 7 rue Soyouz, 87068 Limoges, France

³ Univ. Bordeaux, CNRS, LOMA, UMR 5798, F-33400 Talence, France

Corresponding authors: maher.hamdi@cea.fr, emmanuel.abraham@u-bordeaux.fr

THz radiation can be employed to characterize the dielectric constant and loss tangent of ceramic materials widely used for industrial applications. However, a key parameter in ceramic material production concerns the control of the porosity since it is directly related to the ceramic properties. The evaluation of the ceramic porosity can be achieved by mercury injection. However, THz radiation can propose an alternative effective contact-less and non-destructive approach. In this communication, we focus our attention on alumina (Al₂O₃), the most important, widely used and cost effective oxide ceramic material [1]. We investigate the THz dielectric properties of alumina ceramic samples with porosity fractions from 0% to 20%. Samples are prepared by pressing and sintering 1 μ m grain sizes. Sample porosity was first characterized by the mercury porosimetry technique. Then, THz spectra were obtained with a commercial THz time-domain spectrometer.

For different porosity fractions, Fig. 1 shows the evolution of both the permittivity (a) and the loss tangent (b) from 0.3 to 2 THz. Main interesting feature is that we observe a clear 20% decrease of the sample permittivity as the porosity fraction changes from 0% to 20%. Simultaneously, the dielectric loss strongly increases for samples with higher porosity fractions. At macroscopic scale, the effective properties of a multi-phase composite material can be accurately computed using the properties and the relative fractions of its components. Using the effective medium theory with most common models, we predict the sample permittivity for all porosity fractions from 0% to 20% with a good agreement with the experiment (Fig. 1c). Assuming a spherical aspect for the pores (empty spaces between alumina inclusions), we conclude that the inclusions have also a quasi-spherical shape with an aspect ratio estimated to 0.87.

In the communication, we will also demonstrate that THz time-domain spectroscopy can differentiate alumina samples fabricated with different grain sizes, or reveal a small fraction of impurities, such as 5% ZrO₂, embedded in non-porous alumina. These results demonstrated the potential of THz radiation for non-destructive characterization of low loss high dielectric constant ceramics.

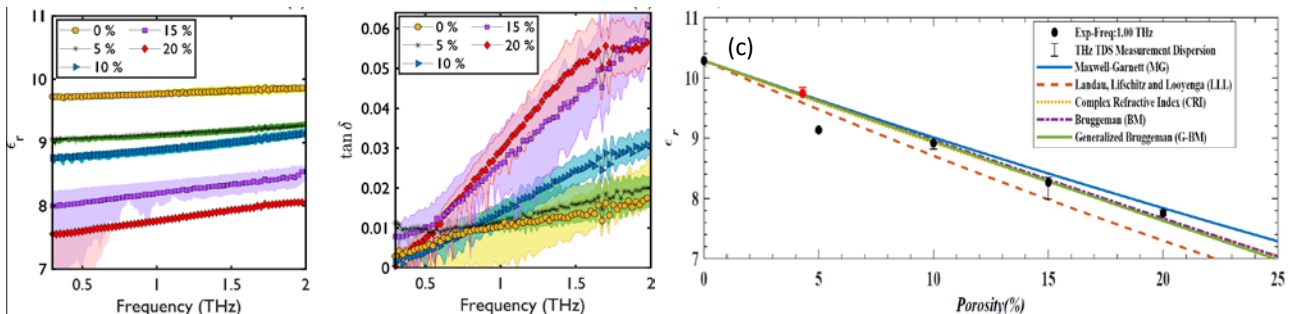


Fig. 1: Dielectric properties of $d_{50}=1 \mu\text{m}$ grain size alumina samples with different porosity fractions. (a) Relative permittivity. (b) Loss tangent. (c) Comparison between experimental relative permittivity of the samples (black dots) and the one predicted from EMMs (solid lines), at 1 THz and as a function of the sample porosity fraction.

[1] K.Z. Rajab et al., "Broadband dielectric characterization of aluminum oxide (Al₂O₃)", J. Micr. El. Pack, 5 (1), 2-7 (2008).

MIR and THz Spectroscopy with 10 nm spatial resolution

Philip Schaefer*, Artem Danilov, Andreas Huber

neaspec GmbH, Munich, Germany

**Corresponding author: philip.schaefer@neaspec.com*

Scattering-type scanning near-field optical microscopy (s-SNOM) is a method that circumvents the diffraction limit of light by creating an optical nano-focus at the apex of a metallic AFM tip, confining the light-matter interaction to the tip-sized optical near-field [1]. This principle works for light from the visible and IR up to the THz spectral range. An asymmetric interferometric detection scheme allows background-free monochromatic optical mapping of amplitude and phase (reflection and absorption) [2] as well as nano-FTIR spectroscopy using a broadband MIR laser source [3], both at 10 nm spatial resolution. THz amplitude and phase spectra are acquired through a coupled THz-time-domain spectrometer.

In this talk, we will show how this AFM-based method can be used for correlative nanoscopy combining optical imaging and spectroscopy with standard scanning probe modes to extensively characterize matter. The broadband optics make it possible to perform optical correlation at the MIR and the THz spectral range and the AFM platform enables the correlation with mechanical data channels, such as AFM topography, as well as electronic AFM modes, such as Kelvin probe force microscopy (KPFM). An example of such correlation can be seen in Fig 1. The left image shows the SRAM structure in topography. High doping concentrations ($10^{18} - 10^{20} \text{ cm}^{-3}$) are highlighted through the IR image and low concentrations ($10^{15} - 10^{17} \text{ cm}^{-3}$) are highlighted through the THz image. Applying the Drude model, charge carrier concentrations and charge mobilities can be determined respectively. Additionally, the Kelvin probe force image (KPFM) maps the surface work function correlatively. With the unique ability to quantify the charge carrier concentration in a contact-free manner from s-SNOM images [4] these correlative measurements can be used for a comprehensive characterization of the surface and nanostructure electronic properties.

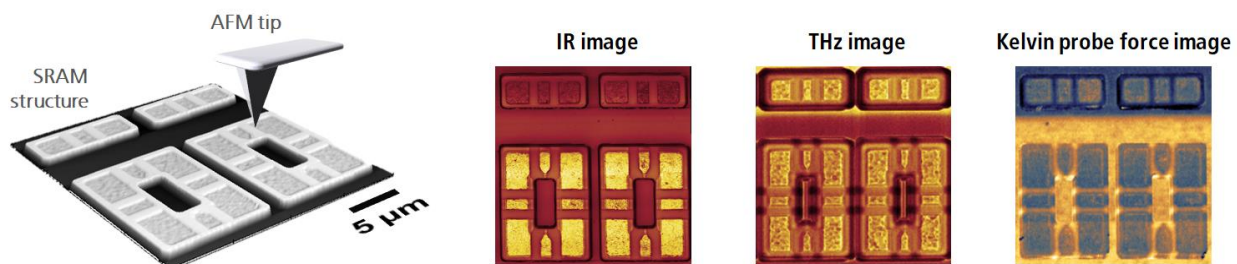


Fig. 1: AFM topography, IR reflection, THz reflection and KPFM nanoscale images of an SRAM structure

References:

- [1] F. Keilmann, R. Hillenbrand, *Phil. Trans. R. Soc. A* 362, 787 (2004).
- [2] N. Ocelic *et al.*, *Appl. Phys. Lett.* 89, 27 (2006)
- [3] I. Amenabar *et al.*, *Nat. Commun.* 8, 14402 (2017)
- [4] C. Liewald, *et al.*, *Optica* 5, 159 (2018)

Multimodal vibrational infrared spectroscopy from 1.1 to 6.5 μm with Aluminum Bowties

M. Najem[§], F. Carcenac[@], F. Gonzalez-Posada[§], T. Taliercio[§]

[§]IES, Univ Montpellier, CNRS, Montpellier, France

[@]LAAS, CNRS, Toulouse, France

Corresponding author: melissa.najem@umontpellier.fr

Vibrational surface-enhanced spectroscopy is a promising application in the plasmonics field, where metallic nanoantennas (NA) are tailored to provide local electromagnetic field localization and enhancement for biomedical applications. [1] To cover a wide IR active range, from 1.1 to 6.5 μm , Al NA were picked as low-cost material with promising optical quality, CMOS compatible, and excellent properties for sensing. Figure A shows a metal-insulator-metal (MIM) with respective thicknesses of 100 nm of Al, 20 nm of SiO_2 , and 50 nm Al NAs.

Figure B shows the single unit cell of the NAs array formed of Al Bowties (BTs). To investigate the spectral response of these periodic Al-BTs, a numerical FDTD solver (Lumerical) was employed, where Maxwell's equations were discretized in both time and space. The Al-BT array was always polarized along y-axis to enhance the electrical field, as the gap strongly localizes the field. [2] For a wide-coverage purpose and to tune their localized surface plasmon resonance (LSPR) at different spectral positions, the side length (L) of each Al-triangle was swept from 0.3 to 2 μm with a step of 0.1 μm (Fig.C). The distance, d, between these triangles was maintained at 100 nm. For each L value, one main plasmonic resonance peak was detected which is usually referred to as a strong dipolar coupling. This first-order plasmonic resonance is always situated at the highest wavelength, then higher orders of resonance and other diffraction peaks appear representing the periodicity triggered along y-axis.

Al-BTs array were fabricated by electron-beam lithography followed by metallization and lift-off process; then were characterized under 36x IR Fourier Transform IR (FTIR) spectrometer. Figure D shows a good agreement between simulation (FDTD) and experimental (FTIR). The detected LSPR peaks appear at the exact simulated spectral position. Such a result is extremely encouraging for a lab-on-chip detection vision of functional groups and fingerprints of any bio-molecule in this propitious IR range using a single plasmonic platform.[3]

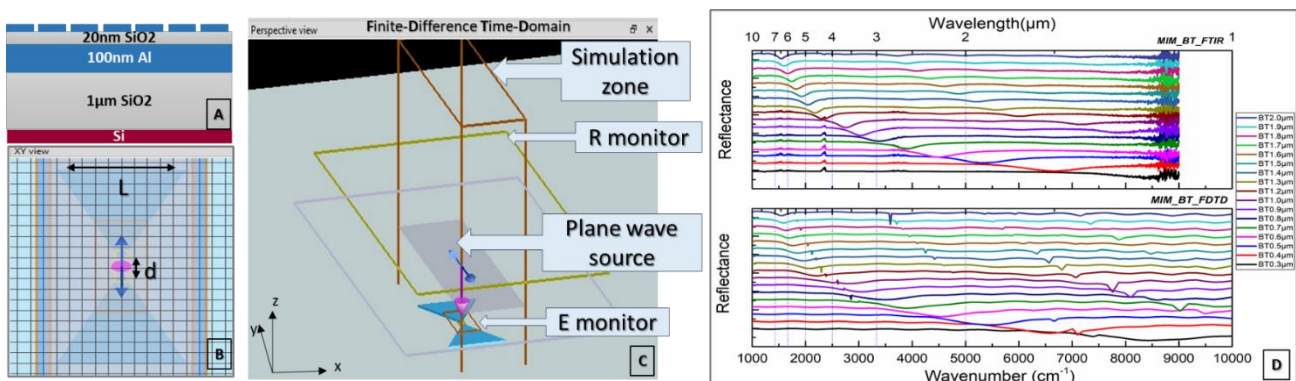


Fig. 1: A) Epitaxial layers from the substrate to the nano-structured Al-BT. B) XY top view from Lumerical simulation software. C) Perspective view of all simulation monitors wrapping up the Al-BT. D) FTIR measurement and Lumerical simulation results of all Al-BTs array sizes.

References:

- [1] B. Cerjan *et al.* ACS Photonics 3, 354–360 (2016).
- [2] B. Wang *et al.* Plasmonics 15, 609–621 (2020).
- [3] F. B. Barho *et al.* Nanophotonics, 7, 507–516 (2017).

Acknowledgements:

This work is partially supported by:

- Equipex EXTRA (ANR-11-EQPX-0016)
- MUSE – PRIME@MUSE – I-Site
- French RENATECH network

Thermal radiation of a single pair of subwavelength antennas

Loubnan Abou-Hamdan¹, Riad Haidar², Valentina Krachmalnicoff¹, Patrick Bouchon², and Yannick De Wilde¹

¹Institut Langevin, ESPCI Paris, PSL University, CNRS, 1 rue Jussieu, F-75005 Paris, France

²DOTA, ONERA, Université Paris-Saclay, F-91123 Palaiseau, France

Corresponding author: loubnan.abou-hamdan@espci.fr

Understanding fundamental interactions between a small number of thermally excited subwavelength antennas is an essential step to optimize the emission of large-scale metasurfaces. The very weak thermal radiation emitted by such systems of nano-antennas, can be extracted by highly sensitive techniques, such as thermal radiation scanning tunneling microscopy [1], and infrared spatial modulation spectroscopy (IR-SMS) [2]. Here, we characterize the far-field thermal emission of a single asymmetric pair of coupled subwavelength metal-insulator-metal (MIM) patch antennas separated by a nanometric gap g , using the IR-SMS technique [3]. The sample geometry and experimental technique are sketched in Fig.1 (a).

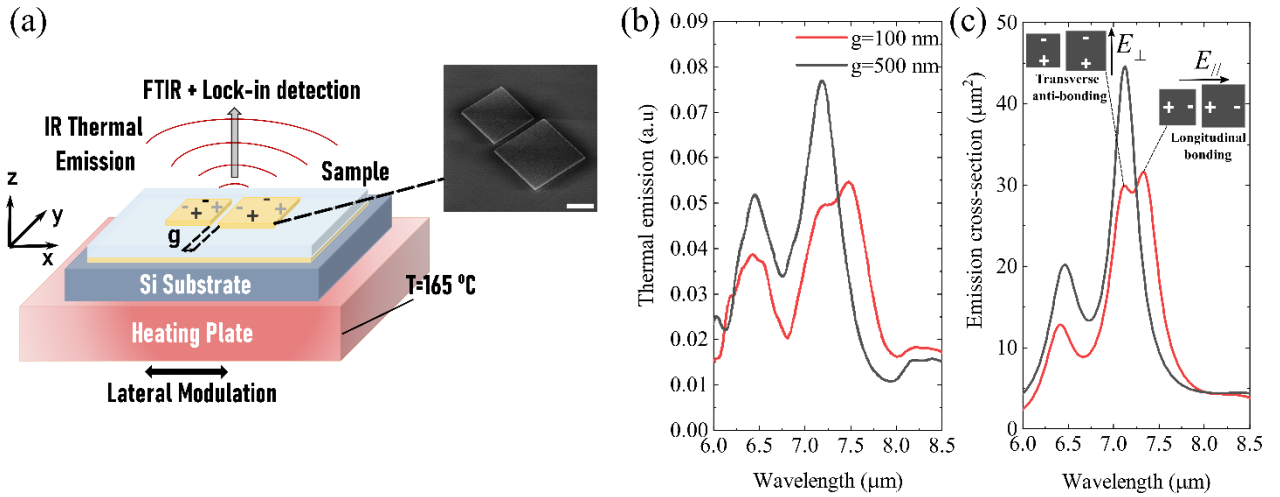


Fig. 1: (a) Schematic illustration of the sample geometry and of the IR-SMS technique. An SEM image of the considered antenna pair is shown in the inset. The scale bar is 1 μm . (b) Measured thermal emission spectra of the antenna pair for different gaps g . (c) FDTD calculations of emission cross-sections corresponding to the measurements. The inset shows a sketch of the dimer geometry showing two of the hybrid modes of the coupled antennas, for electric field polarizations parallel and perpendicular to the dimer axis. The positive (+) and negative (-) signs indicate the surface charge distribution.

As the gap size is reduced to 100 nm (Fig 1(b) and (c), red curve) the two gold patches of the MIM antennas form a dimer pair and a splitting starts to form in the resonance peak between 7 and 8 μm . The observed splitting is a direct result of the simultaneous excitation of the hybrid bonding and anti-bonding modes of the dimer [4], shown in the inset of Fig 1(c). This striking result shows that various coupled modes of a single nano-antenna can be simultaneously excited by thermal fluctuations, an incoherent process arising from fluctuating thermal currents.

The observed interactions in a single pair of thermally excited antennas may guide future efforts to build antenna systems or arrays for various applications.

References:

- [1] Y. De Wilde et al. *Nature*, vol. 444, no. 7120, pp. 740–743, 2006.
- [2] C. Li et al. *Physical Review Letters*, vol. 121, no. 24, p. 243901, 2018.
- [3] L. Abou-Hamdan et al. *Optics Letters*, vol. 46, no. 5, pp. 981–984, 2021.
- [4] P. Nordlander et al. *Nano Letters*, vol. 4, no. 5, pp. 899–903, 2004.

Cd_{1-y}Zn_yTe ternary alloys: from thermodynamic computations to stoichiometric growth conditions

Sara MODNI*¹, Jean Louis SNTAILLER¹, Timotée JOURNOT¹, Gilles PATRIARCHE², Vincent DESTEFANIS³

¹ CEA Leti, LMP, Grenoble

² CNRS, C2N, Palaiseau

³ Lynred, Grenoble

*Sara.modni@cea.fr

Infrared sensors using II-VI materials are well known for various space applications. Their good electrical and optical properties allow high-resolution detection in all IR bands. The detection part of those sensors is composed of a Cd_{1-y}Zn_yTe substrate (CZT) used to grow a lattice-matched layer of Hg_{1-x}Cd_xTe (MCT) (cf. Fig 1). This work will focus on the CZT substrate, with the aim of studying the relation between the second phase defects of the Cd_{1-y}Zn_yTe, the intrinsic defects, and the growth conditions during single crystal elaboration. The understanding of the growth mechanisms may help to reduce these defects and thus improve the crystalline quality of the Hg_{1-x}Cd_xTe active layer grown on top. The improvement of the quality of Cd_{1-y}Zn_yTe and then of Hg_{1-x}Cd_xTe materials will contribute to a better image quality of IR detectors.

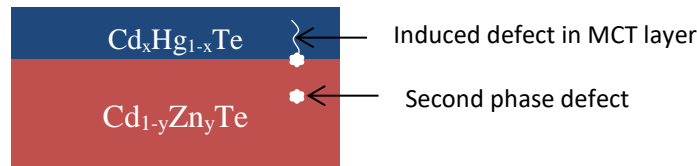


Figure 1 Sketch of the stack of the materials used to make the detection circuit.

The second phase defects (precipitates) are due to the deviation from the stoichiometry during the growth and cooling phases of crystallization. It is therefore important to understand the Cd-Zn-Te ternary phase diagram. The partial pressure of Cadmium, the growth and annealing temperatures and the initial composition of the feedstock are key parameters that must be controlled [1]. For this purpose, a thermodynamic study of the CdTe, ZnTe and Cd_{1-y}Zn_yTe phase diagrams are investigated and will be presented. Now optimized control of partial pressure of components during the growth are tested and CZT second phase defects are measured with a set of characterization methods in order to evaluate the suggested growth conditions.

[1] Vapor pressure scanning of non-stoichiometry in Cd_{0.9}Zn_{0.1}Te and Cd_{0.85}Zn_{0.15}Te. J.H. Greenberg, V.N. Guskov

Large HgTe nanocrystals for THz technology

Thibault Apretna¹, Sylvain Massabeau¹, Charlie Gréboval², Nicolas Goubet², Sukhdeep Dhillon¹,
Francesca Carosella¹, Robson Ferreira¹, Emmanuel Lhuillier², Juliette Mangeney¹

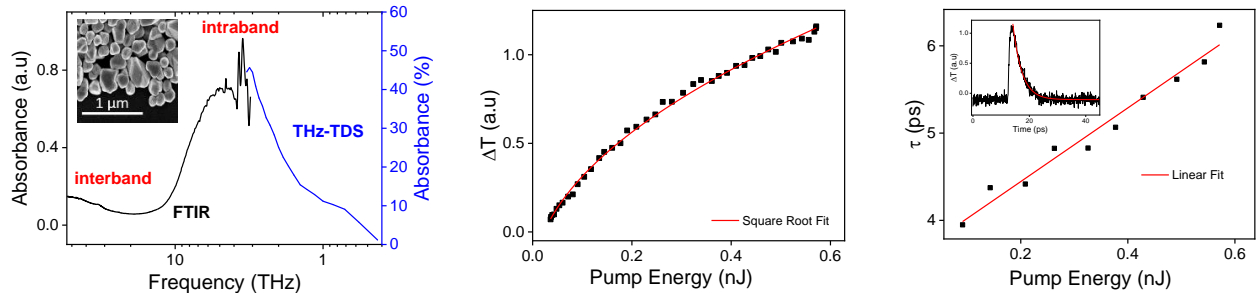
¹Laboratoire de Physique de l'École Normale Supérieure, ENS, Université PSL, CNRS, Sorbonne
Université, Université Paris-Diderot, Sorbonne Paris Cité, Paris France

²Sorbonne Université, CNRS, Institut des NanoSciences de Paris, 4 place Jussieu, 75005 Paris, France

Corresponding author: thibault.apretna@phys.ens.fr

Whereas only few materials can address interband or intersublevel absorption in the THz range, some absorption features at high THz frequencies have been recently demonstrated in large HgTe nanocrystals (of typical size 200 nm) [1]. Indeed, important progress has been obtained on colloidal growth, resulting in a tunable long wavelength absorption peak at THz frequencies. Such HgTe nanocrystals are very attractive for applications since they are low cost and extremely easy to produce [2]. To exploit their potential for THz technology, it is crucial to investigate their optical properties in the full THz frequency range and to get knowledge on the relaxation dynamics of non-equilibrium carriers in these nanocrystals.

Here we process large HgTe nanocrystals (~100 nm size), using colloidal synthesis [1] and study their optical properties in the THz spectral range. We show that their absorbance spectrum, reported in Fig. 1.a., exhibits a broad absorption at high energy (>30 THz) arising from interband transitions and a strong resonance centered at ~4 THz [3]. Using an effective mass model of doped HgTe nanocrystals demonstrate that the observed resonance at ~4 THz is well described by single carrier intraband transitions. We further study the properties of the HgTe nanocrystals at THz frequencies under optical excitation at 800 nm wavelength using an optical pump-THz probe experiment. The differential transmission amplitude ΔT of the THz probe pulse with and without optical pumping follows a root-square law with the incident pump energy (see Fig. 1.b). The dynamics of ΔT , (see insert of Fig. 1.c), as a function of the pump-probe delay are well fitted by a mono-exponential decay law. We extract hot carrier relaxation time τ that increases from 4 ps up to 6 ps as the pump energy is increased (see Fig. 1.c).



Figures : (a) Absorbance spectra of HgTe nanocrystals at room temperature. High frequency spectrum has been obtained using FTIR measurements while low frequency spectrum has been measured using THz-TDS. Insert: SEM Image of large HgTe nanocrystals. (b) Differential transmission amplitude ΔT as a function of the incident pump energy. (c) Extracted carrier relaxation time τ as a function of the incident pump energy. Insert: Measured differential THz transmission ΔT as a function of the pump-probe delay. The red line represents mono-exponential decay law.

Our study uniquely reveals a large THz absorption relying on single carrier intraband transition in HgTe nanocrystals of ~100 nm size. We also demonstrate a hot carrier relaxation time in the range of few ps, demonstrating the great potential of these large HgTe nanocrystals for the development of advanced THz optoelectronic devices.

References:

- [1] N. Goubet et al. "THz HgTe Nanocrystals: Beyond Confinement", *J. Am. Chem. Soc.*, 140, 5033 (2018).
- [2] E. Lhuillier and P. Guyot-Sionnest, "Recent Progresses in Mid Infrared Nanocrystal Optoelectronics". *IEE J. Sel. Top. Quantum Electron.* 23, 1-8 (2017).
- [3] A. Jagtap et al. "Emergence of Intraband Transitions in Colloidal Nanocrystals" *Opt. Mater. Express*, 8, 1174 (2018).

VERTICAL MULTILAYER STRUCTURES BASED ON POROUS SILICON LAYERS FOR MID-INFRARED APPLICATIONS

S. Meziani¹, M. Duris¹, M. Guendouz¹, N. Lorrain¹, P. Pirasteh¹, L. Bodiou¹, W. Raiah^{1,2}, Y. Coffinier², V. Thomy² and J. Charrier^{1,*}

¹Univ Rennes 1, CNRS, Institut Foton – UMR 6082, F-22305 Lannion, France

²Institut d'Electronique, de Microélectronique et de Nanotechnologie (IEMN, UMR CNRS 8520), Avenue Poincaré, BP 60069, 59652 Villeneuve d'Ascq, France.

Corresponding author: joel.charrier@univ-rennes1.fr

The implementation of a Mid-InfraRed (Mid-IR) silicon (Si) photonic transducer with broad Mid-IR transparency (up to 8 μm by taking into account Si transparency) is a challenge that could find applications in spectroscopic sensing and environmental monitoring. This paper demonstrates the fabrication of vertical porous silicon (PSi) multilayer structures on Si substrates and their sensing potential in the Mid-IR wavelength range notably near the cut-off band of Si due to its absorption up to 8 μm . Bragg reflector and vertical cavity on P⁺ silicon substrates for applications in spectroscopic sensing in the Mid-IR wavelength range are fabricated and optically characterized. The complex refractive index of PSi single layers is measured. Optical vertical devices are then fabricated and characterized by Fourier Transform InfraRed (FTIR) spectrophotometry. This work demonstrates the use of electrochemically prepared Bragg reflectors with reflectance as high as 99% and vertical cavity based on PSi layers (figure 1a) operating in the Mid-IR spectral region (up to 8 μm). Experimental reflectance spectra of the vertical cavity structures (figure 1b) are recorded as a function of air exposure duration after thermal annealing under nitrogen flux (N₂) and results demonstrate that these structures could be used for spectroscopic sensing applications in the Mid-IR (2-8 μm) by grafting specific biomolecules on the PSi internal surface and by fabricating optical integrated waveguides.

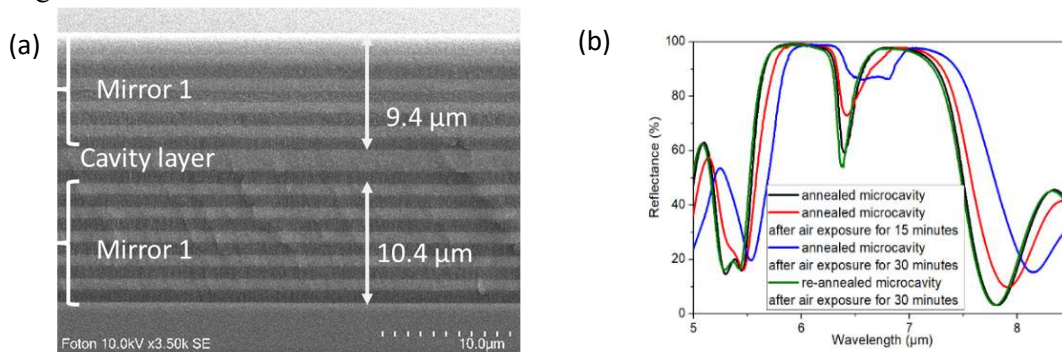


Figure 1: (a) Scanning electron microscope micrograph (cross section) of vertical micro-cavity and (b) Evolution of the experimental reflectance spectra of the same micro-cavity structure as a function of exposure duration to air after annealing at 300°C of the structure under N₂.

Acknowledgments

This work was supported by the French national research agency under MID-VOC ANR project (ANR-17-CE09-0028-01) and by PHC Maghreb project (PHC-2021-45995). Equipment funding of Institut Foton were partly provided by the CPER Sophie. Scanning Electron Microscopy imaging and porous silicon fabrication were performed in the CCLLO - Renatech clean room facilities of Institut Foton. The PhD grants of S. Meziani by Allocations de recherche doctorale (CDO and CD22) are gratefully acknowledged. Maxime Duris acknowledges financial support from ANRT (Association Nationale Recherche Technologie) through a CIFRE grant N°2015/1042.

Quantum cascade detectors operating in the strong light-matter coupling regime.

M. Lagrée^{@\$}, G. Quinchard^{@*}, M. Jeannin^{§*}, O. Ouznali[§], A. Bousseksou[§], V. Trinité[@],
R.Colombelli[§], A. Delga[@]

[@] THALES Research and Technology, Campus Polytechnique, 1, Avenue Augustin Fresnel, RD 128, 91767 Palaiseau cedex, France
[§] Centre de Nanosciences et de Nanotechnologies (C2N), CNRS UMR 9001, Université Paris-Saclay, 91120 Palaiseau, France

* contributed equally

Corresponding author: mathurin.lagree@3-5lab.fr

Infrared detectors operating in the mid-IR spectral range (3 μm -20 μm) find applications in the field of spectroscopy, space observation, free space telecommunication and imaging. Detectors based on intersubband (ISB) transitions are of major interest for both applicative and fundamental aspects, as they feature high sensitivity and high speed. Usually operated in the weak light-matter coupling regime, quantum cascade detectors (QCD) [1], photo-voltaic counterparts of quantum well infrared detectors (QWIP), provide also an interesting playground to study fundamental aspects of the strong light-matter coupling regime.

Over the past decade, there have been continuous research efforts to develop MIR and THz emitters based on ISB polaritons, quasi particles arising from the strong light-matter coupling between an ISB transition and a photonic micro-cavity mode, as they are predicted to have improved functionalities with respect to current sources [2,3]. However, efficient electrical injection of polaritonic devices is a major challenge, with few experimental demonstrations present in the literature [4]. The reason is that most of the electrons injected from an electronic reservoir into a polaritonic system tunnel into dark states [2].

To get insightful information on the transport mechanisms underlying the tunnel coupling process, it is of interest to study the inverse process [5]: the extraction of an electrical current from a polaritonic reservoir, i.e. a detection process. We investigate the photo-response of MIR QCDs ($\lambda = 10\mu\text{m}$) operating in the strong light-matter coupling regime ($2\Omega \approx 10 \text{ meV}$). This is particularly relevant, as it allows to study the process of *resonant* current extraction from a polaritonic state into an electric state. By measuring the optical absorption and the photocurrent (Fig. 1(a)), we are able to experimentally retrieve an effective (polariton) extraction efficiency. We develop an intuitive, semi-classical formalism based on the coupled modes theory (CMT) which quantitatively reproduces both the optical and electrical device characteristics. The excellent agreement between the experimental data and our simplified transport model confirms previous reports on QWIP detectors operating in the strong-coupling regime [5]. We also show that the current extraction involves electronic tunnelling from the polaritonic state to the extractor state, and thus that the dark electronic states do not contribute to the photocurrent (Fig. 1(b) and (c)).

These results highlights the potential of QCDs to study ISB-polaritonic systems, and establish an intuitive picture of the polaritonic extraction. They constitute a step towards a better understanding of the resonant electrical injection of carriers into a polaritonic state for efficient ISB polaritonic emitters.

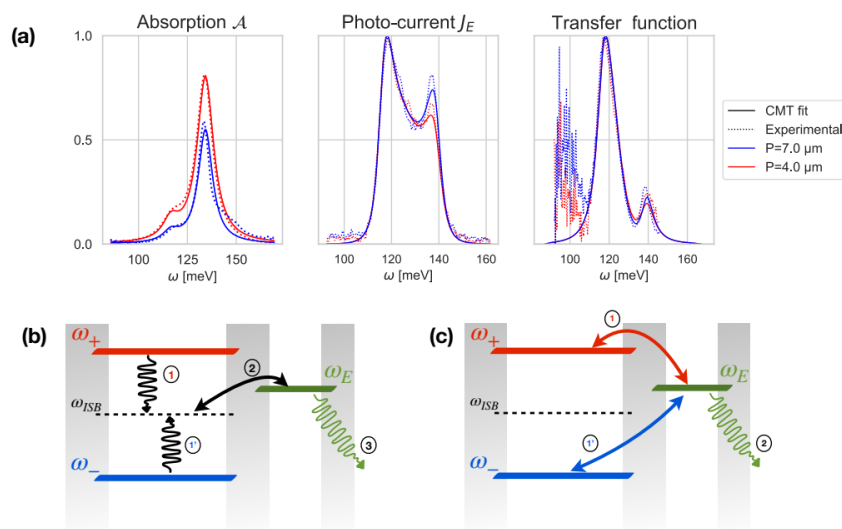


Fig. 1: (a) Left and center: absorption and normalized photo-current, and CMT fit. Right : polaritonic transfer function deduced from the measurements.

Two possible extraction scheme :
(b) Intrasubband dominated transport : polaritons collapse into the dark states before extraction.
(c) Tunnelling through polaritonic states:

References:

- [1] Gendron, L., Carras, M., Huynh, A., Ortiz, V., Koeninguer, C., & Berger, V. (2004). Quantum cascade photodetector. *APL*, 85(14), 2824-2826.
- [2] De Liberato, S., & Ciuti, C. (2008). Quantum model of microcavity ISB electroluminescent devices. *Phy. Rev. B*, 77(15), 155321.
- [3] Colombelli, R., & Manceau, J. M. (2015). Perspectives for intersubband polariton lasers. *Physical Review X*, 5(1), 011031.
- [4] Sapienza, L., Vasanelli, A., Colombelli, R., Ciuti, C., Chassagneux, Y., Manquest, C., ... & Sirtori, C. (2008). Electrically injected cavity polaritons. *Physical review letters*, 100(13), 136806.
- [5] Vignerot, P. B., Pirota, S., Carusotto, I., Tran, N. L., Biasiol, G., Manceau, J. M. & Colombelli, R. (2019). *APL* 114(13), 131104.

Coating Thickness Mapping Extraction by Time-Domain Terahertz Spectroscopy

Q. Cassar^{1,2}, F. Fauquet¹, J.P. Guillet¹, M. Maurès², J.B. Perraud² & P. Mounaix¹

¹Integration from Material to Systems Laboratory, University of Bordeaux, 33405, Talence, France

²Optikan SAS, 2b Rue du Maréchal Joffre, 33260, La Teste de Buch, France

Corresponding author: jean-baptiste.perraud@optikan.com

quentin.cassar@u-bordeaux.fr

The thickness of the coating layers is one of the most important quality factors in the aerospace industry. Nowadays, a number of methods exist that can quantify the thickness of coatings. However, none of them are suitable for determining the respective thickness of coatings deposited in layers on non-metallic substrates. With the development of robust systems, time-domain terahertz spectroscopy has proven to be a candidate of choice to complete the arsenal of usual methods to control the thicknesses of multi-coatings. In many cases, the study of the time of flight of multiple reflections at the dielectric interfaces of each coating allows the estimation of the thicknesses. However, when studying micrometric layers, the time of flight of the various reflections is too short to adopt such a strategy. Indeed, the multiple interactions at the interfaces give rise to a complex signal presenting the superposition of the individual contributions. To overcome such complexity, we have developed an algorithmic approach combining a previously published work, the Iterative Tree Algorithm (ITA) with specific objective function minimization, with the aim of retrieving the individual thicknesses of aeronautic coating stacks. Each layer composing a training stack was preliminary calibrated in isolation to extract its dielectric profiles. The intrinsic properties such as the refractive index and the extinction coefficient were tested for each coating, by reconstructing the topography of a deposit in isolation. These measurements were correlated with the results provided by the eddy current method (Figure 1). Following the calibration step, the estimation of individual thicknesses on a real deposit of several overlapping coatings was performed. The results were found to be consistent with a destructive optical measurement. Finally, these investigations are thought to provide the essential steps for the design of terahertz tools for the control of the thickness of different coatings present in a stack.

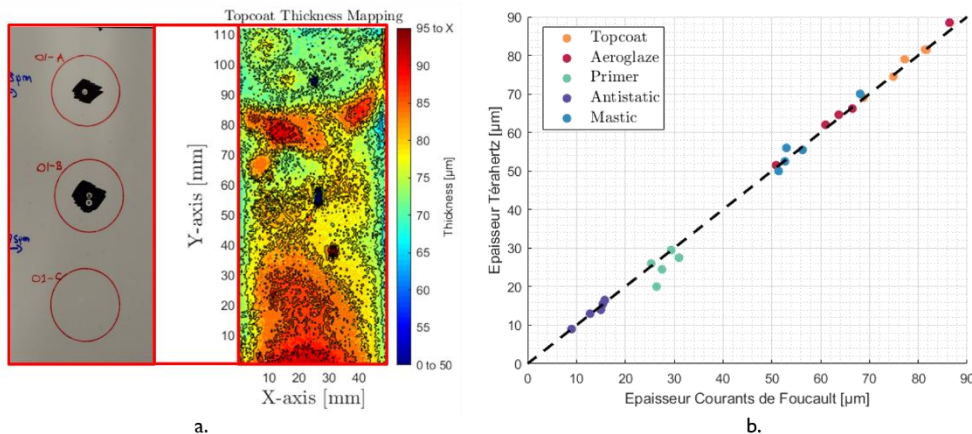


Fig. 1: a. Photograph and terahertz thickness map of a coating in isolation for calibration. b. Comparison between terahertz and eddy current thickness at different location for different coating in isolation.

References:

[1] Q. Cassar et al., "Iterative Tree Algorithm to Evaluate Terahertz Signal Contribution of Specific Optical Paths within Multi-Layered Materials," IEEE Transactions on Terahertz Science and Technology, vol. PP, no. c, pp. 1–1, 2019.

Terahertz refractive index-based morphological dilation: A strategy towards improving breast conserving surgery

Q. Cassar^{1,2}, S. Caravera³, G. MacGrogan³, T. Bücher⁴, P. Hillger⁴, U. Pfeiffer⁴, T. Zimmer¹,
J.P. Guillet¹ & P. Mounaix¹

¹Integration from Material to Systems Laboratory, University of Bordeaux, 33405, Talence, France

²Optikan SAS, 2b Rue du Maréchal Joffre, 33260, La Teste de Buch, France

³Department of Pathology, Bergonié Institute, 33076, Bordeaux, France

⁴Institute for High-Frequency and Communication Technology, University of Wuppertal, 42119, Wuppertal, Germany

Corresponding author: quentin.cassar@u-bordeaux.fr

Preliminary investigations have shown that breast cancer tissues have higher refractive index profiles than healthy tissues in the terahertz band [1]. However, these variations were observed for tissues with a structural homogeneity of about 90%. Thus, when studying areas where the structural homogeneity is drastically lower than the one aforementioned -typically around the tumour area-, the refractive index alone does not allow a rigorous demarcation between healthy and malignant tissue. As a result, it raises delicate question on the exact spatial extent of the tumour. In order to facilitate the spatial delineation of the tumour, a pixel-by-pixel classification based on the extraction of the tissue refractive index map, directly after surgery, followed by morphological dilation was investigated [2]. The method consists of establishing an initial diagnosis based on the refractive index of each pixel at 550-GHz by means of an inverse electromagnetic problem. A refractive index threshold is then defined so that pixels exhibiting a refractive index higher than the threshold are classified as malignant while others are considered as benign pixels. The preliminary classification is followed by morphological dilation. Such a process is operated from pixels previously classified as malignant. Hence, malignant zones are progressively spread over the neighbourhood. Doing so allows one to overcome the aforementioned class-overlapping limitations. A schematic of the process is given in Fig. 1, for an arbitrary dilation shape. The respective confusion matrices, as well as the receiver operating characteristic curves for each combination of a refractive index threshold and dilation shapes, have been extracted. For the best case, the process of morphological dilation enhanced the effectiveness of the diagnosis by about 33%. Diagnosis images will be presented and discussed during the presentation.

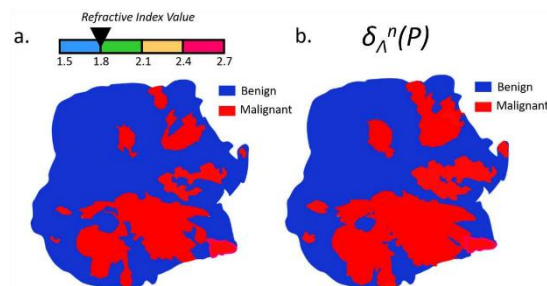


Fig. 1: Principle of morphological dilation applied on a tissue binary refractive index map. a: Binary refractive index map set at 1.8. b: Morphological dilation applied to the binary refractive index map with an arbitrary dilation operator.

References:

- [1] Ashworth, P. C., Pickwell-MacPherson, E., Provenzano, E., Pinder, S. E., Purushotham, A. D., Pepper, M., & Wallace, V. P. (2009). Terahertz pulsed spectroscopy of freshly excised human breast cancer. *Optics express*, 17(15), 12444-12454.

[Type the document title]

[2] Cassar, Q., Caravera, S., MacGrogan, G., Bücher, T., Hillger, P., Pfeiffer, U., ... & Mounaix, P. (2021). Terahertz refractive index-based morphological dilation for breast carcinoma delineation. *Scientific reports*, 11(1), 1-16.

THz acquisition and rendering with augmented reality

Jean-Paul Guillet[@], Frédéric Fauquet[@], Patrick Mounaix[@]

^{@IMS Laboratory, University of Bordeaux, UMR CNRS 5218, Bat A31 351 cours de la Libération, 33405 TALENCE}

Corresponding author: jean-paul.guillet@u-bordeaux.fr <https://terahertz.fr>

NON-DESTRUCTIVE testing at terahertz frequencies has benefited in recent years from advances in semiconductor technologies (Si-based and III-V-based technologies), whose frequencies have been able to move from millimetric frequencies to terahertz. There are now commercially available terahertz radars. Applications of such non-destructive testing systems are for example composite materials inspection [1] or art painting diagnosis [2]. Moreover, even if some THz handled system were demonstrated [3-4], they do not allow a direct non-contact scan and we cannot see directly the image during the acquisition.

The experimental setup, illustrated on figure 1, combines an integrated wideband FMCW radar (122 GHz to 170 GHz), two 3" lenses with 115 mm focal length and a smartphone using a reality augmented interface. A metal plate (4x8cm) is placed below the painting at the mouth location. In this first demonstration, an intermediate processing step is performed between the radar and the smartphone using a computer. A Fourier transform and then the extraction of the amplitude corresponding to the position of the painting is sent to the smartphone as an analog voltage. After a first phase of calibration where we have to scan rapidly all the painting in order to generate a virtual mapping, we can move the system freely and see a THz image appearing on the phone screen with a color gradient which is superimposed on the painting (see Figure 2). It is necessary to stay in the Rayleigh zone (1cm) to have a homogeneous image. For this, a distance measurement based on camera image guide the experimenter during the acquisition, and an articulated arm can also be used to control the distance. A post measurement application allows then to see the results in augmented reality directly in the smartphone. This makes it possible to move, including with all the degrees of angular freedom, and to see the THz image either superimposed on the object, or by hovering a few centimeters from the object.

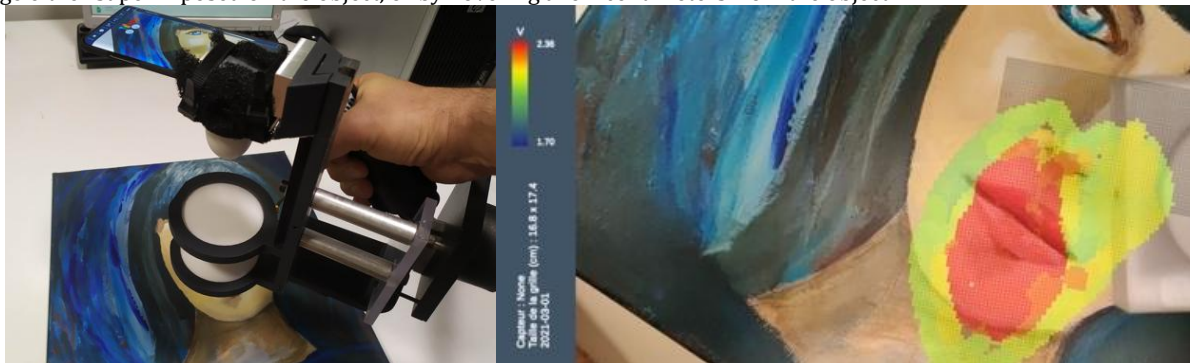


Figure 1 : (left) Photography of the experiment. A painting is manually scanned using the AR-THz system. (right) Screenshot of the mobile application with a superimposition of the camera view and the THz image

The feasibility of AR-THz using FMCW imaging system is proven. A good match between the spatial resolution of the manual scan assisted by the smartphone and the resolution of the radar makes it possible to quickly obtain information on the analyzed object, with the possibility of seeing it in augmented reality. Radar signal processing in the computer is still a limitation at this time, but it could be integrated in the smartphone in the future, and for example thickness measurement or synthetic Aperture radar techniques.

REFERENCES

- [1]. Pan, M., Chopard, A., Fauquet, F., Mounaix, P., & Guillet, J. P. (2020). Guided Reflectometry Imaging Unit Using Millimeter Wave FMCW Radars. *IEEE Transactions on Terahertz Science and Technology*, 10(6), 647-655.
- [2]. Guillet, J. P., Wang, K., Roux, M., Fauquet, F., Darracq, F., & Mounaix, P. (2016, September). Frequency modulated continuous wave terahertz imaging for art restoration. In *2016 41st International Conference on Infrared, Millimeter, and Terahertz Waves (IRMMW-THz)* (pp. 1-1). IEEE.
- [3]. Duling III, I. N. (2016, May). Handheld THz security imaging. In *Image Sensing Technologies: Materials, Devices, Systems, and Applications III* (Vol. 9854, p. 98540N). International Society for Optics and Photonics.
- [4]. Ellrich, F., Bauer, M., Schreiner, N., Keil, A., Pfeiffer, T., Klier, J., ... & Molter, D. (2020). Terahertz quality inspection for automotive and aviation industries. *Journal of Infrared, Millimeter, and Terahertz Waves*, 41(4), 470-489.

THz imaging of injection-mold weld lines in ABS thermoplastic

Min Zhai, Alexandre Locquet, D.S. Citrin[@]

Georgia Tech-CNRS IRL2958, Georgia Tech Lorraine, 2 Rue Marconi, 57070 Metz, France
School of Electrical and Computer Engineering, Georgia Institute of Technology, Atlanta, Georgia,
30332-0250 USA

Corresponding author: david.citrin@ece.gatech.edu

Stagnating weld lines, a common defect in injection-mold thermoplastic products, form where two separate melt fronts impinge head-on and after which there is no subsequent flow. The presence of weld lines will degrade the mechanical properties of injection-mold products significantly. To date, the most common approach used to identify weld lines is destructive mechanical testing. In this work, terahertz (THz) reflective imaging and scanning acoustic microscopy (SAM) were utilized for material characterization as well as quality control of an injection-mold thermoplastic electrical receptacle plate.

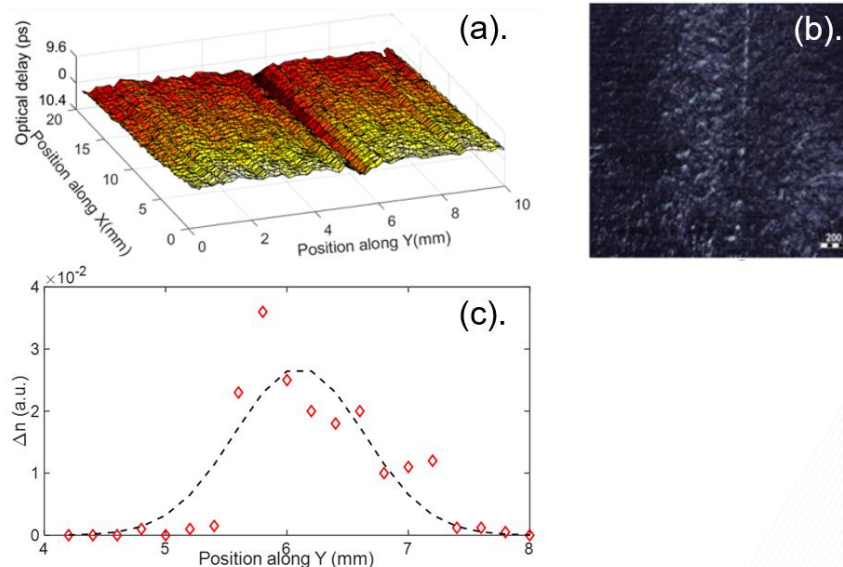


Fig. 1. (a). THz C-scans based on the peak reflected signal arrival time used as contrast mechanism. (b). SAM micrographs operating at center frequency $f=420$ MHz. (c). Birefringence along a section perpendicular to weld line.

The surface morphology of the injection-mold plastic samples was characterized using THz reflective imaging and SAM, shown in Fig. 1 (a)-(b). V-shaped weld lines are observed clearly in both THz and SAM results, and its corresponding width and depth are ~ 400 μm and ~ 10 μm , respectively.

Owing to the microstructure of weld lines, birefringence which corresponds to the magnitude of anisotropy, is also worthy of study. Spatially dependent THz birefringence is observed in Fig. 1 (c). We find that enhanced THz birefringence is localized around the weld line, and decreases gradually with the distance away from the weld line, demonstrating that the anisotropic state related to the frozen-in molecular orientation and internal stress transforms to isotropic state as the ABS moves away from the weld line. Micro-elastic heterogeneity resolved in acoustic micrographs validates the location-dependent birefringence observed in THz results.

References:

- [1] M. Zhai et al., "Diagnosis of injection-molded weld lines in ABS thermoplastic by polarized terahertz reflective imaging," submitted to NDT&E Int.
- [2] E.T. Mohamed et al., "Scanning acoustic microscopy investigation of weld lines in injection-molded parts manufactured from industrial thermoplastic polymer," *Micron*, 138:102925, 2020.
- [3] G.H. Oh et al., "Terahertz time-domain spectroscopy of weld line defects formed during an injection moulding process," *Compos. Sci. Technol.*, 157:67-77, 2018.

Accounting for the pellet's porosity in THz-TDS measurements of powder oxides

Jaume Calvo-de la Rosa^{1,2}, Alexandre Locquet^{2,3}, Denis Bouscaud⁴, Sophie Berveiller⁴, and D.S. Citrin^{2,3}

¹ *Department of Condensed Matter Physics, Faculty of Physics, IN2UB, Universitat de Barcelona, Martí i Franquès 1, 08028, Barcelona, Spain*

² *Georgia Tech-CNRS UMI 2958, Georgia Tech Lorraine, 2 Rue Marconi, 57070, Metz, France*

³ *School of Electrical and Computer Engineering, Georgia Institute of Technology, Atlanta, GA, 30332-0250, USA*

⁴ *Laboratoire d'Etude des Microstructures et de Mécanique des Matériaux LEM3 (UMR CNRS 7239), Arts et Métiers ParisTech, Université de Lorraine, 4 rue Augustin Fresnel, 57078, Metz, France*

Corresponding author: jaumecalvo@ub.edu

Terahertz time-domain spectroscopy (THz-TDS) is every time a more popular technology to study the optical and dielectric properties of materials in the THz frequency range, typically from 0.1 THz to 10 THz. Materials such as explosives, drugs, organic, ceramic or composites are commonly studied by THz-TDS. However, due to the high attenuation that many of these materials have, it is common to work with powder materials dispersed into a THz-transparent matrix (typically polyethylene, PE).

Despite this is a very common practice, the experimental implementation needs to be carefully done and requires a detailed interpretation of the data in order to avoid other effects to appear, leading to an error on the property's deduction. Some of these non-intrinsic effects are size dependencies (i.e., powder – bulk different behaviour), the relative volume between powder and matrix (known as *filling factor*, f_v), scattering, or percolation between particles, for instance. Many of these effects can be accounted by using Effective Medium Models (EMMs), which are commonly used to extract the pure powder's properties from the measured properties of the mixture.

Nonetheless, the porosity contained inside the pellet (within the PE matrix, for instance) is not considered by the EMMs and it is often forbidden in THz-TDS works. However, if the porosity level is high, this might have an important effect on the measured properties due to the large permittivity difference between air and the powder materials typically investigated. In this work we propose a methodology based on a sequential two-step' implementation of EMMs to quantify the contribution of the porosity on THz-TDS measurements on CuO and ZnO powder samples.

Our algorithm considers the pellet as a ternary system (powder + PE + air) instead of a binary one (powder + PE). Contrary to previous works, which solve this problem by applying three-phases implementations of a single EMM (such as Maxwell-Garnett or Bruggeman), our approach is capable to adapt to each phase physical characteristics and uses a specific model for each phase. Our results show very good agreement between experimental data and models and conclude that the most accurate results are obtained by using a combination of the Vegard's law (to account for the porosity) and the Maxwell-Garnett model (to deduce the oxides' properties).

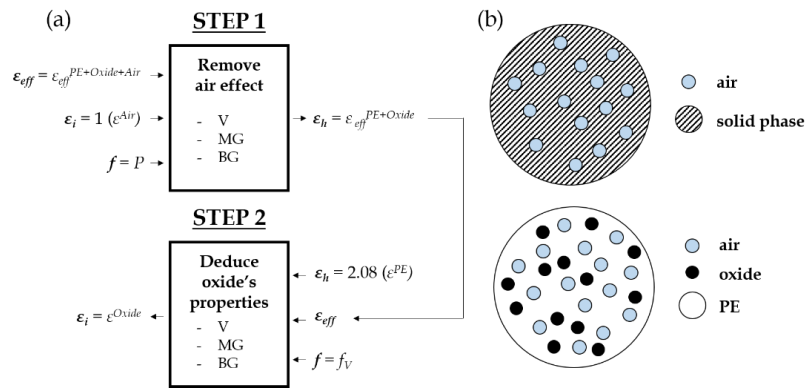


Fig. 1: Scheme of the developed two-steps method based on the combination of two EMMs. Fig. from [2].

References:

- [1] J. Calvo-de la Rosa, *et al.*, *Ceramics International* 46 (15), 24110-24119 (2020).
- [2] J. Calvo-de la Rosa, *et al.*, *IEEE Trans. Terahertz Sci. Technol. Early Access* (2021).

Electroluminescence from HgTe quantum dots and its Use for Active Imaging

Junling Qu[@], Emmanuel Lhuillier[@]

[@] Sorbonne Université, CNRS, Institut des NanoSciences de Paris, INSP, F-75005 Paris, France.

Corresponding author: el@insp.upm.fr

Mercury telluride (HgTe) colloidal quantum dots are among of the most versatile infrared (IR) materials with the absorption of first optical absorption which can be tuned from visible to the THz range. Therefore, they have been extensively considered as near IR emitters and as absorbers for low-cost IR detectors. However, the electroluminescence of HgTe remains poorly investigated in spite of its ability to go toward longer wavelengths compared to traditional lead sulfide (PbS). Here, we demonstrate a light emitting diode (LED) based on an indium tin oxide (ITO)/zinc oxide (ZnO)/ZnO-HgTe/PbS/gold stacked structure, where the emitting layer consists of a ZnO/HgTe bulk heterojunction which drives the charge balance in the system. This LED has low turn-on voltage, long lifetime, and high brightness. Finally, we conduct short wavelength infrared (SWIR) active imaging, where illumination is obtained from a HgTe NC-based LED, and demonstrate moisture detection.

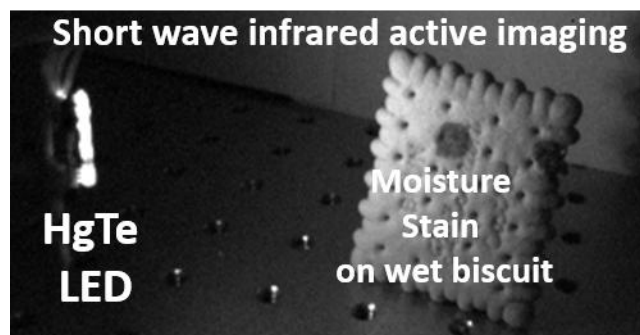


Fig. 1: moisture stain on a wet biscuit revealed by electroluminescence from HgTe quantum dots

References:

- [1] J Qu et al, Nano Letters 20, 6185 (2020)
- [2] Y. Prado et al, Chem Mater 33, 2054 (2021).

Gate tunable colloidal nanocrystal-based infrared sensor

Tung Huu Dang^{*,§}, Angela Vasanelli[@], Yanko Todorov[@], Carlo Sirtori[@], Emmanuel Lhuillier[§]

[@] Laboratoire de physique de l'Ecole Normale Supérieure, ENS, Université PSL, CNRS, Sorbonne Université, Université de Paris, 75005 Paris, France

[§] Sorbonne Université, CNRS, Institut des NanoSciences de Paris, INSP, 75005 Paris, France.

Corresponding author: tung.dang-huu@phys.ens.fr

Photodetectors based on solution-processed active materials, such as colloidal nanocrystals (NCs), have emerged as promising candidates for the next generation of infrared sensing devices. However, these materials suffer from weak light absorption efficiency and poor electrical conductivity due to hopping transport. Here, we integrate HgTe NCs into plasmonic resonators and exploit spoof surface plasmon to enhance NC film absorption in the mid-wave infrared. We show that coupling the plasmonic resonator with the NC film improves the device's performance effectively, with a specific detectivity reaching 8×10^9 Jones at 80 K, while the responsivity is 0.25 A/W at 200 K. Moreover, the device configuration allows us to tune the carrier density by simply applying a gate bias, which leads to an increase of the photocurrent to dark current ratio up to a factor of 20.

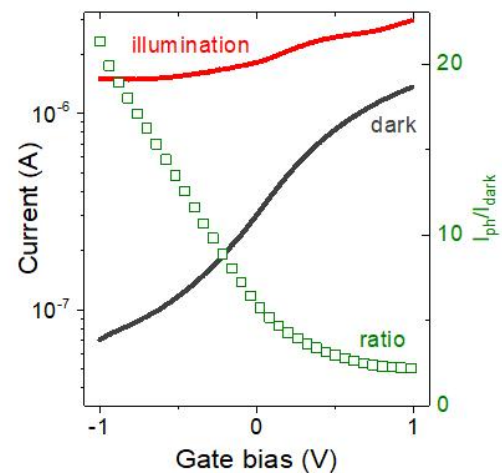
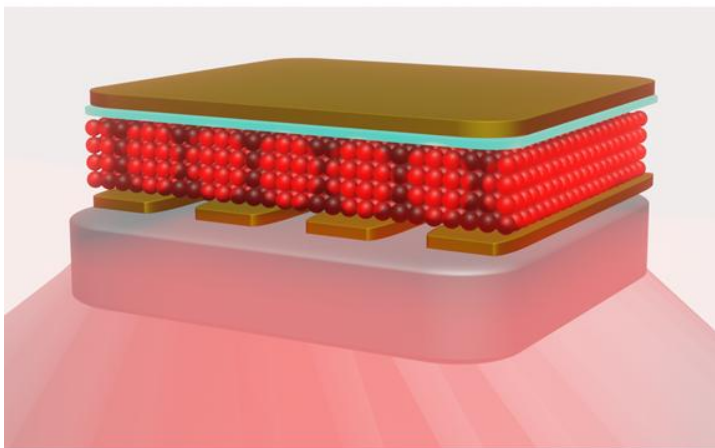


Fig. 1: Left: Scheme of the nanocrystal-based device coupled to a plasmonic cavity. Right: Current in dark conditions (black line) and under illumination (red line) as a function of gate bias. Green symbols present the ratio between the current under illumination and the dark current (right scale).

References:

- [1] C. Gréboval *et al.*, Chem Rev 121, 3627 (2021).
- [2] A. Chu *et al.*, ACS Photonics 6, 2553 (2019).
- [3] D Palaferrri *et al.*, Nature 556, 85 (2018).
- [4] P. Jouy *et al.* Appl. Phys. Lett. 98, 021105 (2011)

Highly sensitive heterodyne detection with stabilized QCL lasers

Mohammadreza Saemian¹, Djamal Gacemi¹, Yanko Todorov¹, Angela Vasanelli¹,
Olivier Lopez², Benoît Darquié², Carlo Sirtori¹

¹Laboratoire de Physique de l'Ecole Normale Supérieure, ENS, Université PSL, CNRS, Sorbonne Université, Université de Paris, 75005 Paris, France

²Laboratoire de Physique des Lasers, Université Sorbonne Paris Nord (Université Paris 13), CNRS, Villetaneuse, France

Corresponding author: Mohammadreza.saemian@phys.ens.fr

QCLs are semiconductor lasers based on inter subband transition in the conduction band of semiconductors. They are promising continuous wave light sources (c.w.) in the MIR range (from 3 to 25 μ m). However, their frequency stability is limited by many different external sources of noise and therefore the typical free-running linewidths are in the MHz level, partially limited by the noise that arises from electrical current fluctuations [1]. Their frequency fluctuations can be controlled by comparing to a reference, and by generating a correction signal to apply to the injection current [2].

In this work, we demonstrate the active stabilization of a DFB-QCL to another DFB-QCL by using a phased-lock loop (PLL) correction system, fabricated at the LPL laboratory. For this aim, we used two QCLs (one as a Local Oscillator and the other as the Signal, 96 and 47 mW respectively) and measured the heterodyne beating (up to 800MHz) of the two lasers on a fast commercial photodetector (VIGO). The RF beating is compared to a RF stable reference signal and the PLL is used to actively change the injection current of the Signal laser allowing us to stabilise the relative beatnote between the two lasers at the Hz level. Fig. 1 shows the power spectral density (PSD) of the beating for different beatnote frequencies. We achieved a signal to noise ratio of nearly 50 dB at 1Hz of RBW. Our results demonstrate that by active stabilization of QCLs and benefiting from phase correction with PLL box, it is possible to lock the frequency of one laser to another without any long-term drift. This method opens the way to the highly sensitive heterodyne detection with NEP in the fW range, while the heterodyne receiver is kept at 300 K [3].

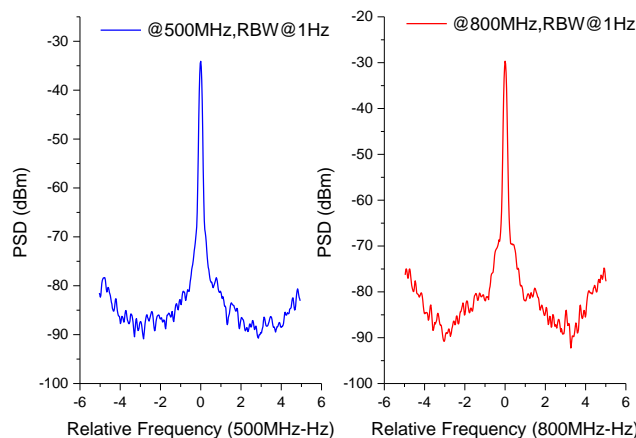


Fig. 1: Beatnote signals between two QCLs, one being phase-locked to the other.

References:

- [1] L. Tombez et al. Optic Lettres, Vol. 38, issue 23, pp.5079-5082 (2013).
- [2] B. Argence et al. Nature Photonics 9, 456-460 (2015).
- [3] D. Palaferri et al., Nature, vol. 556, no. 7699, pp. 85–88, Mar. 2018

Hot Carrier Semiconductor Plasmonic Mid-infrared Photodetector

A. Haky¹, A. Vasanelli¹, Y. Todorov¹, D. Gacemi¹, G. Beaudoin², K. Pantzas², I. Sagnes², C. Sirtori¹

¹Laboratoire de Physique de l'Ecole normale supérieure, ENS, Université PSL, CNRS, Sorbonne Université, Université de Paris, 75005 Paris, France

²Centre for Nanosciences and Nanotechnology, CNRS, Université Paris-Saclay, UMR 9001, 10 Boulevard Thomas Gobert, 91120, Palaiseau, France

Corresponding author: andrew.haky@ens.fr

Plasmonic nanostructures have recently been used to enhance the light-matter interaction and to improve the quantum efficiency of internal emission Schottky photodiodes [1]. When the plasmonic mode is used to both enhance the electric field and absorb the radiation, the device is termed a hot carrier photodetector [2]. Hot carrier plasmonic photodetection has so far been reported for nanostructures which support surface plasmon modes [3].

Here we demonstrate a semiconductor plasmonic hot carrier detector in the mid-infrared which uses a volume plasmon mode, the well-known Berreman mode [4], as the absorbing medium. The Berreman mode is a collective electronic resonance supported by an electron gas in a slab with thickness smaller than the plasma wavelength. The semiconductor acts as a quasi-monochromatic perfect absorber for a critical coupling angle [5]. We detect a resonant photocurrent signal at the frequency of the plasmon mode when a small DC bias is applied to the device. We demonstrate that the same device emits radiation at the plasmon frequency under the excitation of a modulated electric pulse.

Our system is an ideal platform to study the long-standing problem of the interaction of a single particle current with a collective electronic excitation [6]. Importantly, the mature InP platform used in this study allows for the engineering of the band structure which may help to elucidate the microscopic processes involved in the energy transfer between the collective mode and the single particle electrons.

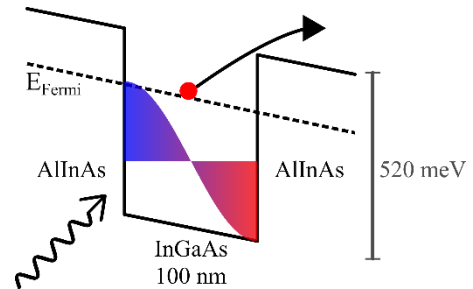
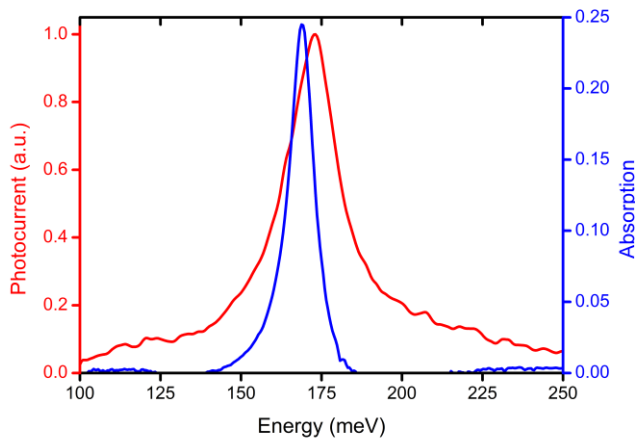


Fig. 1: The normalized absorption (300K) and photocurrent spectra (7K) for a 100 nm InGaAs layer doped with an electronic density of $2e19 \text{ cm}^{-3}$. The collective dipole associated with the Berreman mode is sketched with the electronic band structure.

References:

- [1] M. W. Knight et al. *Science*, vol. 332, no. 6030, pp. 702–704, May 2011.
- [2] A. Dorodnyy et al. *IEEE J. of Selected Topics in Quantum Electronics*, 24, 6, pp. 1–13, Nov. 2018
- [3] M. L. Brongersma et al. *Nature Nanotechnology*, 10, 1, pp. 25–34, Jan. 2015
- [4] B Askenazi et al., *New J. Phys.* 16, 043029 (2014)
- [5] A. Vasanelli et al., *Nanophotonics*, vol. 10, no. 1, pp. 607–615, Sep. 2020
- [6] T. Laurent et al. *Appl. Phys. Lett.*, vol. 107, no. 24, p. 241112, Dec. 2015

Mid-infrared frequency comb for QCL stabilisation and detectors assessment at $9\mu\text{m}$

Livia Del Balzo¹, Djamel Gacemi¹, Yanko Todorov¹, Angela Vasanelli¹, Benoit Darqui  ², Olivier Lopez², Carlo Sirtori¹

¹ Laboratoire de Physique de l'Ecole Normale Sup  rieure, ENS, Universit   PSL, CNRS, Sorbonne Universit  , Universit   de Paris, Paris, France

² Laboratoire de Physique des Lasers, Universit   Sorbonne Paris Nord (Universit   Paris 13), CNRS, Villetaneuse, France

Corresponding author: djamal.gacemi@phys.ens.fr

The mid-infrared (MIR) spectral region has numerous scientific and technological applications. In recent years even more applications have been empowered by the emergence of quantum cascade lasers (QCLs) as compact, reliable and commercially available semiconductor sources that can deliver up to hundreds of mW at room temperature. QCL technology lacks convenient metrological implementation such as frequency comb generation and frequency stability at the sub-Hz level, which would have a tremendous impact for applications that need extreme accuracies [1]. Moreover, detectors in MIR frequency range are much less performing than at shorter wavelength. Their sensitivity could be enormously improved by implementing coherent heterodyne detection scheme [2].

In the present work, we demonstrate the phase-stabilization of a MIR QCL source to a novel $9\mu\text{m}$ frequency comb originating from a femtosecond mode-locked fiber laser. This MIR comb system has been commercially supplied by MenloSystems. By beating a DFB-QCL with one of the comb tooth on a fast QCD detector, we were able to phase-stabilize the resulting relative beat-note signal at the Hz level (Fig1a), and thus to copy the spectral performance of the MIR comb to the QCL. By measuring the beating of the comb teeth, we also demonstrated the electrical bandwidth optical characterisation of a quantum detectors (Fig1b).

In the future we are aiming to combine this stabilized QCL with a quantum detector to demonstrate the most sensitive heterodyne detection system that will endow applications such as high-resolution spectroscopy, coherent LIDAR measurements, test and design of systems for free-space coherent optical communications with GBits/s data transfer rate.

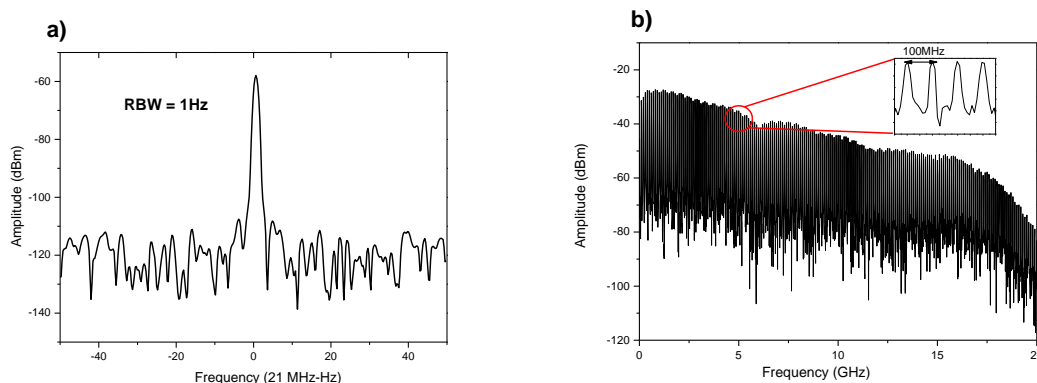


Figure 1 : a) Beatnote signal between the QCL and one tooth of the novel MIR comb when the QCL is phase-locked to the comb tooth. b) Harmonics of the MIR comb with a frequency repetition rate of 100MHz measured on a quantum cascade detector.

References:

- [1] B. Argence *et al.* *Nat. Photonics*, vol. 9, no. 7, pp. 456–460, Jun. 2015.
 [2] D. Palaferri *et al.*, *Nature*, vol. 556, no. 7699, pp. 85–88, Mar. 2018.

Optimizing patch antenna arrays for MIR quantum detectors

Etienne Rodriguez¹, Thomas Bonazzi¹, Hamza Dely¹, Azzurra Bigoli¹, Angela Vasanelli¹, Yanko Todorov¹, Carlo Sirtori¹

¹Laboratoire de Physique de l'Ecole Normale Supérieure, ENS, Université PSL, CNRS, Sorbonne Université, Université de Paris, 24 rue Lhomond, 75005, Paris, France

Corresponding author: Etienne.rodriguez@phys.ens.fr

The development of devices based on Intersubband Transitions (ISBT) revolutionized the emission and detection in the mid-infrared region ($\lambda=5\mu\text{m}-20\mu\text{m}$). Thanks to its unique properties, ISBT allow a remarkable degree of freedom for the choice of the emission and detection wavelength, a high-speed behavior, and a high saturation threshold due to short carrier lifetime. [1]–[5] Quantum Well Infrared Photodetectors (QWIP) or Quantum Cascade Detectors (QCD) using conventional mesa show good results in the Mid-Wavelength Infrared (MWIR) region and Long-Wavelength Infrared (LWIR) region. [6], [7] However, these performances have been greatly improved using patch-antenna properties: QWIPs or QCDs embedded into a metamaterial made of subwavelength doubled-metal patch antenna resonators strongly enhance the performances up to room temperature. [8]–[10] In this work we provide a comprehensive analysis of various device parameters in order to achieve an optimized patch-antenna array according to the applications required.

The large number of geometrical parameters (periodicity, height, size...) and optical parameters (refractive index, absorption wavelength, doping concentration...) make the optimization a difficult task. We have combined numerical methods (finite element simulations) with an analytical approach such as Coupled Mode Theory (CMT) in order to quantify the interaction between the QWs and the antenna resonator as well as to extract various loss rates directly from the reflectivity curves. [11] Our approach allows us to link the losses of our systems with our constraints, i.e., handling the amount of light coupled in our system (radiative loss) and its dissipation in the contact or the QWs (non-radiative losses). This work will allow us to increase the performances of our photodetectors and unlock further experimental work such as ultra-strong coupling and laser emission using patch-antenna Quantum Cascade Lasers (QCL).

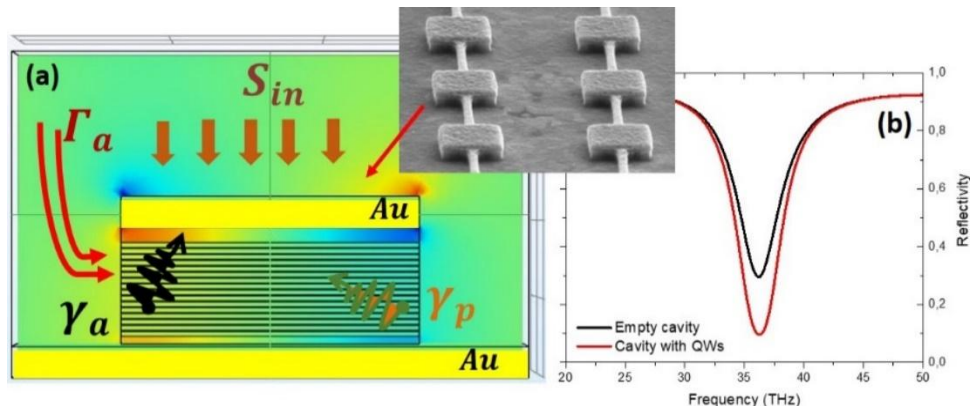


Fig. 1: (a) Simulation of an infinite array of patch with the important parameters displayed; Γ_a (radiative loss), γ_a (non-radiative loss in the contact), γ_b (non-radiative loss in the ISBT) and S_{in} (incoming light).

(b) Reflectivity spectra of the simulations with and without absorption in the QWs. Inset: Electronical image of the device.

References:

- [1] H. Schneider et H. C. Liu, *Quantum well infrared photodetectors: physics and applications*. Berlin ; New York: Springer, 2007.
- [2] F. Capasso, « Band-Gap Engineering: From Physics and Materials to New Semiconductor Devices », *Science*, vol. 235, n° 4785, p. 172- 176, janv. 1987, doi: 10.1126/science.235.4785.172.
- [3] H. C. Liu, Jianmeng Li, M. Buchanan, et Z. R. Wasilewski, « High-frequency quantum-well infrared photodetectors measured by microwave-rectification technique », *IEEE J. Quantum Electron.*, vol. 32, n° 6, p. 1024- 1028, juin 1996, doi: 10.1109/3.502380.
- [4] P. D. Grant, R. Dudek, M. Buchanan, et H. C. Liu, « Room-Temperature Heterodyne Detection up to 110 GHz With a Quantum-Well Infrared Photodetector », *IEEE Photonics Technol. Lett.*, vol. 18, n° 21, p. 2218- 2220, nov. 2006, doi: 10.1109/LPT.2006.884267.
- [5] K. L. Vodopyanov, V. Chazapis, C. C. Phillips, B. Sung, et J. S. Harris, « Intersubband absorption saturation study of narrow III - V multiple quantum wells in the spectral range », *Semicond. Sci. Technol.*, vol. 12, n° 6, p. 708- 714, juin 1997, doi: 10.1088/0268-1242/12/6/011.
- [6] A. Rogalski, « Infrared detectors: status and trends », *Prog. Quantum Electron.*, vol. 27, n° 2- 3, p. 59- 210, janv. 2003, doi: 10.1016/S0079-6727(02)00024-1.
- [7] H. Schneider *et al.*, « Dual-band QWIP focal plane array for the second and third atmospheric windows », *Infrared Phys. Technol.*, vol. 47, n° 1- 2, p. 53- 58, oct. 2005, doi: 10.1016/j.infrared.2005.02.028.
- [8] D. Palaferri *et al.*, « Room-temperature nine- μm -wavelength photodetectors and GHz-frequency heterodyne receivers », *Nature*, vol. 556, n° 7699, p. 85- 88, avr. 2018, doi: 10.1038/nature25790.
- [9] A. Bigioli *et al.*, « Mixing Properties of Room Temperature Patch- Antenna Receivers in a Mid- Infrared ($\lambda \approx 9 \mu\text{m}$) Heterodyne System », *Laser Photonics Rev.*, vol. 14, n° 2, p. 1900207, févr. 2020, doi: 10.1002/lpor.201900207.
- [10] A. Bigioli *et al.*, « Long-wavelength infrared photovoltaic heterodyne receivers using patch-antenna quantum cascade detectors », *Appl. Phys. Lett.*, vol. 116, n° 16, p. 161101, avr. 2020, doi: 10.1063/5.0004591.
- [11] M. Jeannin *et al.*, « Absorption Engineering in an Ultrasubwavelength Quantum System », *Nano Lett*, p. 7, 2020.

Room temperature, high speed, mid-infrared Stark-shift modulator on InP

Thomas Bonazzi[@], Hamza Dely[@], Etienne Rodriguez[@], Djamel Gacemi[@], Yanko Todorov[@], Konstantinos Pantzas[§], Grégoire Beaudoin[§], Isabelle Sagnes[§], Angela Vasanelli[@], Carlo Sirtori[@]

[@]Laboratoire de Physique de l'Ecole Normale Supérieure, ENS, Université PSL, CNRS, Sorbonne Université, Université de Paris, 24 rue Lhomond, 75005, Paris, France

[§]Centre de Nanosciences et de Nanotechnologies (C2N), CNRS—Université Paris-Sud/Paris-Saclay, Palaiseau 91120, France
Corresponding author: thomas.bonazzi@ens.fr

Highly sensitive and ultrafast mid-infrared optoelectronic systems¹ are required for free-space communications², light detection and ranging (LIDAR), high resolution spectroscopy and in observational astronomy.

In this work we present a high-speed room temperature InP-based external modulator at 9 μm . The device is based on a system of *n*-doped asymmetric coupled GaInAs/AlInAs quantum wells grown by MOCVD on an InP substrate. When applying a bias on the device, the transition energy between states 1 and 2 is submitted to a linear Stark shift. The absorption can thus be put in and out of resonance with respect to a fixed laser frequency^{3,4} (see left panel of Fig. 1). The absorption can be tuned over more than 40 meV with fields < 70kV/cm, allowing to switch between a transparent and an absorptive configuration (see right panel of Fig. 1) with a highly linear behaviour. Note that the modulation is not performed by depleting electron concentrations. The device is therefore characterized by an intrinsically large bandwidth and very low electrical power consumption (\sim few mW) with respect to direct laser modulation. In order to take advantage of this intrinsically ultrafast modulator, special care was taken to process this quantum structure into a RF-compatible device able to operate up to several GHz⁵. We report here 47% modulation depth for our modulator, which shows bandwidths of up to tens of GHz. The limit in modulation speed appears to be eventually limited by the packaging of the device and not by the underlying physics, showing the great potential of this concept for high bitrate data transmission.

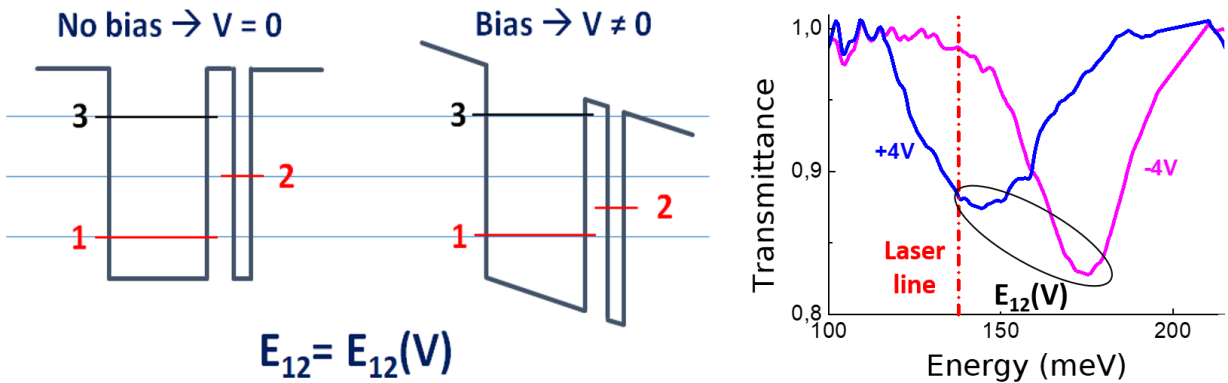


Fig. 1: Left: Conduction band diagram illustrating the Stark-shift of E_{12} transition, tunable with an external electric field. Right: Transmission spectra under bias. At positive bias (blue) the laser light is absorbed while under negative bias (pink) the modulator becomes transparent.

References:

- [1] F. Capasso *et al.*, IEEE JOURNAL OF QUANTUM ELECTRONICS **38**, 511 (2002)
- [2] X. Pang *et al.*, Phys. Status Solidi A **218**, 2000407 (2021)
- [3] C. Sirtori *et al.*, Appl. Phys. Lett. **60**, 151–153 (1992).
- [4] J. Teissier *et al.* Optics Express **20**, 1172 (2012)
- [5] E. Rodriguez *et al.*, ACS Photonics **5**, 3689–3694 (2018)

Strong Anti-correlation in a Quantum Cascade Laser Frequency Comb

B.Chomet¹, F.Kapsalidis², H. Dely¹, D. Gacemi¹,
A. Vasanelli¹, Y.Todorov¹, J.Faist², C.Sirtori¹

¹ *Laboratoire de Physique de l'Ecole normale supérieure, ENS, Université PSL, CNRS, Sorbonne Université, Université de Paris, Paris, France*

² *Institute for Quantum Electronics, ETH Zurich, 8093 Zürich, Switzerland*
baptiste.chomet@phys.ens.fr

Frequency combs (FC) have found tremendous utility as precision instruments in domains ranging from frequency metrology [1], optical clocks [2], broadband spectroscopy [3] and ranging [4]. While in literature FC are mostly linked to ultra-fast lasers that emit short pulses, Quantum Cascade Lasers (QCLs) were shown to rather generate a frequency modulated combs whose intensity was thought to remain constant [5]. In contrast to ultra-fast lasers, the generated FM comb in QCLs is appealing for fundamental laser science and molecular spectroscopy. While the QCL's comb nature has been rigorously proven through the Shifted Wave Interference Fourier Transform Spectroscopy (SWIFTS) [6], the correlations among spectral lines and noise have yet to be explored.

Here we demonstrate the presence of strong anti-correlations among two spectral portions of a standard monolithic Fabry-Perot QCL that operates in the FC regime. The laser under study is a standard ridge 6mm QCL, operating at 290K in continuous wave at a wavelength of $\sim 8.5\mu\text{m}$ with maximum output power of 100mW. The recorded optical spectra (Fig.1 (a)) shows two spectral lobes separated in frequency by ~ 0.6 THz. Applying the SWIFTS technique to this FC we were able to reconstruct the temporal evolution of the intensity of each lobes over one round trip of the cavity. The result, in Fig. 1(b), shows a strong antiphase dynamics between the two spectral lobes. The laser action associated to Lobe 1 is perfectly anticorrelated with that of Lobe 2, when one is on the intensity of the other is off. This behavior is further confirmed by analyzing the intermodal beat note corresponding to each of the two lobes (Fig. 1(c)).

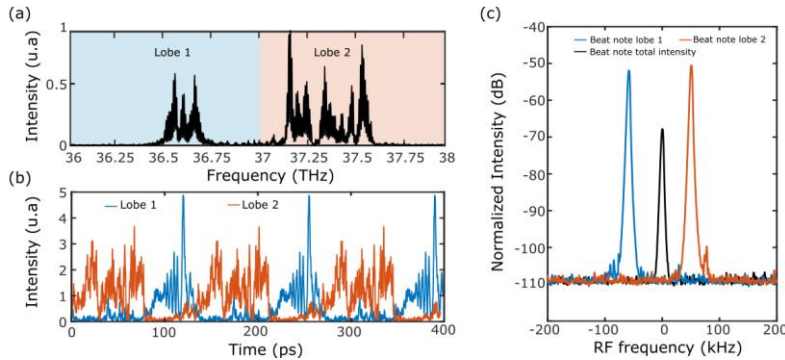


Fig. 1: (a) Optical spectrum of the bilobed QCL (b) SWIFTS reconstructed intensity of each spectral lobes (c) Intermodal beat note of each lobes (blue & red) and of the total intensity (black)

References:

- [1] T. Udem, R. Holzwarth, and T. W. Hänsch, *Nature* 416, 233 (2002).
- [2] S. Diddams, et al., *Science* 293, 825 (2001).
- [3] S. A. Diddams, L. Hollberg, and V. Mbele, *Nature* 445, 627 (2007).
- [4] I. Coddington, W. Swann, L. Nenadovic, and N. Newbury, *Nature Photonics* 3, 351 (2009).
- [5] A. Hugi, G. Villares, S. Blaser, H. C. Liu, and J. Faist, *Nature* 492, 229 (2012).
- [6] M. Singleton, P. Jouy, M. Beck, and J. Faist, *Optica* 5, 948 (2018).

High bitrate Free-Space Optical communication at 9 μm wavelength using Unipolar Devices operating at room-temperature

H. Dely¹, T. Bonazzi¹, O. Spitz², E. Rodriguez¹, K. Pantzas³, G. Beaudoin³, I. Sagnes³, L. Li⁴, A. Giles Davies⁴, E. H. Linfield⁴, F. Grillot², A. Vasanelli¹ and C. Sirtori¹

¹Laboratoire de Physique de l'ENS, Ecole Normale Supérieure - PSL, F-75231 Paris Cedex 05, France

²Télécom Paris, Institut Polytechnique de Paris, F-91120 Palaiseau, France

³Centre de Nanosciences et Nanotechnologies, Université Paris-Saclay, F-91120 Palaiseau, France

⁴School of Electronic and Electrical Engineering, University of Leeds, Leeds, LS2 9JT, UK

Corresponding author: hamza.dely@ens.fr

Unipolar quantum optoelectronic devices rely only on transitions between electronic states in the conduction band. These devices are promising for high-frequency operation in the mid-infrared due to very fast relaxation times of electrons in the excited states, in the order of few picoseconds [1]. As their operation wavelengths are in the atmospheric transparency windows ($\lambda \sim 4-5 \mu\text{m}$; $\lambda \sim 8-14 \mu\text{m}$), they are suited for long range free-space optical communication at very high-bitrates [2]. Several options are available including direct or external modulation of phase and/or intensity.

In this work we present data transmission results obtained using a setup based on $\lambda = 9 \mu\text{m}$ unipolar devices operating at room-temperature: a continuous wave (CW) quantum cascade laser (QCL), a quantum cascade detector (QCD) [3] with an external intensity modulator based on the quantum-confined Stark effect in between. This modulator is designed to avoid charge displacements in the quantum structure and allows bandwidths up to few tens of GHz. We achieved 8 Gbit.s^{-1} bitrate with a bit error rate (BER) of 10^{-3} which can be corrected with negligible overhead using error correction code (ECC) [4]. To the best of our knowledge, this is an improvement of two orders of magnitude with respect to the state-of-the-art [5].

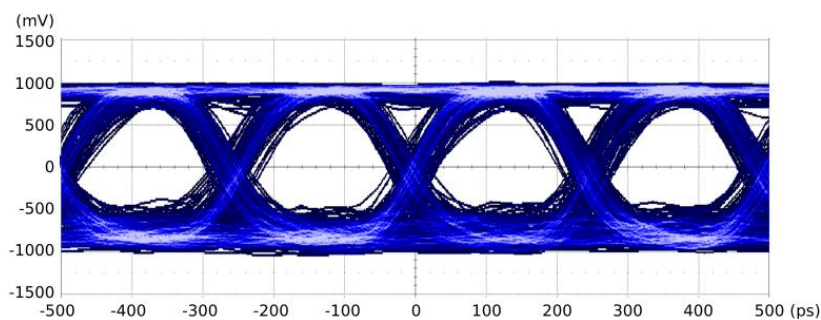


Figure 1: Eye diagram measured at 4 Gbit.s^{-1} with a high-speed oscilloscope used to evaluate the quality of a data transmission. An opened eye showing well-resolved high and low states (ones and zeros) indicates a good transmission quality with a low BER. Here, the BER extracted using the data analysis software of the oscilloscope is lower than 10^{-21} .

References:

- [1] R. Paiella *et al.* Appl. Phys. Lett. 79, 2526 (2001)
- [2] A. Delga and L. Leviandier, Proc. SPIE 10926, 1092617 (2019);
- [3] A. Bigioli *et al.*, Appl. Phys. Lett. 116, 161101 (2020)
- [4] O. Ozolins *et al.* 45th Eur. Conf. on Opt. Comm. (ECOC 2019), pp. 1-4

[5] T. Li et *al.* Photon. Res. 7, 828-836 (2019)

280-GHz Radiation Source Driven by a 1064-nm Dual-Frequency Laser

Alaeddine Abbes[@], Ping-Keng Lu[§], Philippe Nouvel[@], Annick Pénarier[@],
Luca Varani[@], Arnaud Garnache[@], Mona Jarrahi[§] and Stéphane Blin[@]

[@]IES, Univ Montpellier, UMR CNRS 5214, Montpellier FR

[§]University of California Los Angeles, CA, USA

Corresponding author: alaeddine.abbes@umontpellier.fr

We investigate continuous-wave (CW) THz emission using a photoconductive antenna driven by a 1064-nm laser. Only few demonstrations were reported at 1064 nm [1,2], despite the availability and maturity of high-power lasers and components. Here, we combine a CW dual-frequency Vertical-external-cavity emitting laser [3] with a plasmonic-based photomixer [4], all operating at 1064 nm for CW THz generation. The photomixer is fabricated on an epitaxial semiconductor structure consisting of a 200-nm-thick undoped $\text{In}_{0.24}\text{Ga}_{0.76}\text{As}$ layer and a 200-nm-thick AlAs layer grown on a semi-insulating GaAs by molecular beam epitaxy. The photoconductor layer is integrated with a broadband logarithmic spiral antenna and plasmonic contact electrodes. The latter provide sub-picosecond transit time for photo-generated carriers thus enabling photomixing at THz frequencies without using a short-carrier-lifetime substrate.

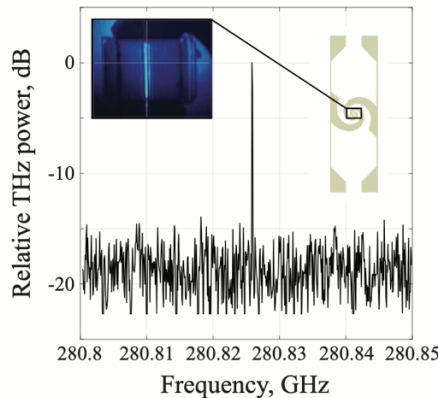


Fig. 1: Measured THz power spectrum around 280 GHz for a resolution bandwidth of 30 kHz. The top left inset shows the optical beam focused in- between plasmonic electrodes connected to the spiral antenna (top right inset).

The dual-frequency laser operation is based on the simultaneous operation of two transverse Laguerre-Gauss (LG) modes, offering a highly-stable and coherent spectrum for any beat frequency in the range 50–900 GHz [3]. These modes are combined by injecting a single-mode fiber. At the fiber output, cylindrical lenses are used to create an elliptical spot beam around the antenna gap (inset image from Fig.1). The THz signal is measured using a calibrated heterodyne head receiver. Figure 1 shows the measured THz power spectrum, clearly indicating a coherent radiation at 280 GHz for an incoming optical power of 30 mW.

This work was supported by ANR *Spatiotera* and C2N french RENATECH network for the DF-VeCSEL.

References:

- [1]. R. Czarny et al., *Proc. SPIE*, vol. 5619, 2004.
- [2]. S. Blin et al., *IEEE J. Sel. Top. Quantum Electron.* **23**(4), 1500511, 2017.
- [3] D. Turan et al., *Optics Express* **28**, 3835-3845, 2020.

Low Optical Power-Driven THz Modulator

Julien Guise*, Stéphane Blin*, Emmanuel Centeno[@] and Thierry Taliercio*

**Institut d'Electronique et des Systèmes, Montpellier, France*

[@]*Institut Pascal, Clermont-Ferrand, France*

Corresponding author: julien.guise@umontpellier.fr

The THz domain is an intense field of research. Nowadays, we notice that many sources (frequency multiplication, QCLs, UTC-PD) and detectors [1] (bolometers, HEMTs, photoconductive antennas) exist. However, only a few modulators are available with low energy consumption and a weak footprint. In this perspective previous works [2] demonstrated the possibility to optically modulate a THz beam running through an InAs slab by photogenerating free carriers. In the continuity of this work, we seek to reduce the required optical power by now operating at 1550 nm in order to benefit from the fiber telecom technology, to have a better control on the beam size and to reach high power densities to obtain very significant effects.

We present here the results of a numerical model implemented on MATLAB in order to try to predict the experiment and to anticipate the different key parameters. Indeed, we show that by reducing the size of the THz beam compared to the initial config. [2] we can then use smaller IR beams to cover the THz beam. These small IR beams allow us to benefit from very high optical densities and we can thus generate much more free carriers in the semiconductor by optical absorption effect. The presence of these carriers allows to reach a quasi-metallic effect of the slab in the desired THz range. We can then modulate the transmission of the THz wave passing through the modulator by switching it between a non-optically-pumped state (dielectric which transmit the THz wave) and an optically-pumped state (metal which reflects the THz).

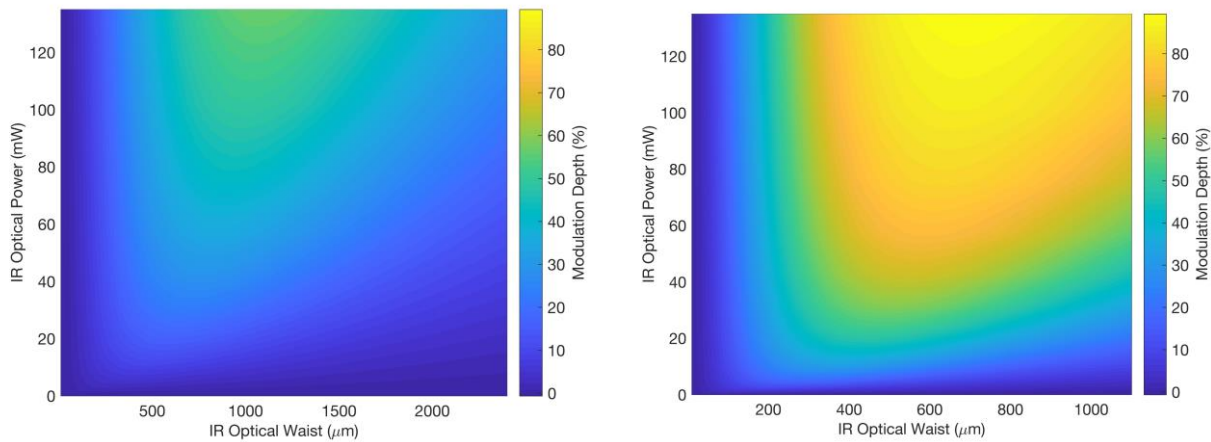


Fig. 1: 2D map of the THz transmission modulation of a 5.5 μm -thick InAs slab for different IR optical waists and IR optical powers for two configurations; (a) THz waist = 1.2 mm and (b) THz waist = 550 μm

As shown in Fig. 1, for a small IR waist, the overlap between the THz and the IR beams is low and therefore the modulation efficiency degrades regardless of IR optical power. At larger IR waist, a higher IR power is required to maintain some modulation efficiency as it depends directly on optical intensity (evolving quadratically with waist). We can see that according to Fig. 1, the initial config. (a) only allows a modulation of the order of 50% (when $w_{\text{opt}} \approx w_{\text{THz}}$ and this in the desired IR power range). We can see that when we decrease the THz waist in config. (b), we can reach up to 90% of the modulation depth of the transmission.

References:

- [1] E. Herrmann et al. J. Appl. Phys. 128, 140903 (2020).
 [2] E. Alvear et al. Appl. Phys. Lett. 117, 111101 (2020).

Acknowledgments : partial funding by the French "Investment for the Future" program (EquipEx EXTRA ANR-11-EQPX-0016)

Polarization control of emitted THz waves using spintronic emitters with anisotropic magnetic layers & birefringence characterization of Quartz

Geoffrey Lezier¹, Pierre Koleják^{1,2}, Jean-François Lampin¹, Kamil Postava², Mathias Vanwolleghem¹ and Nicolas Tiercelin¹

¹Univ. Lille, CNRS, Centrale Lille, Univ. Polytechnique Hauts-de-France, UMR 8520 - IEMN - Institut d'Electronique de Microélectronique et de Nanotechnologie, F-59000 Lille, France

²VSB-Technical University of Ostrava, Nanotechnology centre and IT4Innovations, 17. listopadu 15, 708 33 Ostrava-Poruba, Czech Republic

Corresponding author: geoffrey.lezier@centralelille.fr

The TeraHertz frequency band presents many potential applications in a wide variety of fields, from non-invasive control to spectroscopy. THz spintronic emitters, introduced by Kampfrath et al., offer a new approach to THz wave emission [1]. Exciting a 5d/3d non-magnetic (NM)/ferromagnetic (FM) multilayer by IR fs-pulses generates a spin-polarized current that upon diffusion in the NM metal undergoes strong spin-orbit coupling. The action of the inverse spin-Hall effect transforms the spin-current into a charge current dipole transversely oriented to the spin direction. The polarization state is intrinsically linked to the magnetization direction in the FM layer. Thus, the control of the THz polarization is possible with the rotation of magnetization. Up to now, it was done by rotating the applied magnetic field [2].

The use of a ferromagnetic layer with uni-axial anisotropy allows to coherently rotate the magnetization by varying the applied field ONLY along the hard axis between its saturation values (Fig1.(a)). We deposited a W(2nm)/ FeCo(0.5nm)/ TbCo₂(0.8nm)/ FeCo(0.5nm)/ Pt(2nm) emitter stack on a c-cut Sapphire substrate by RF sputtering in a LEYBOLD Z550 equipment. During the growth, a magnetic field

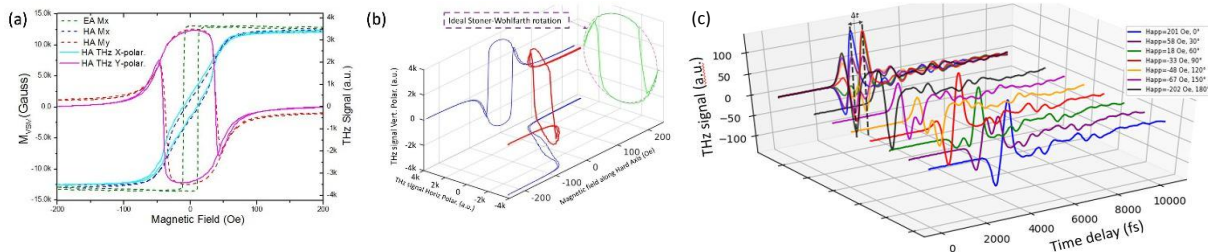


Fig. 1 (a) Comparison between VSM measured magnetic loops (dashed lines) and THz-TDS measurement (full lines) (b) 3D representation of the longitudinal and transversal components of the THz emission vs. magnetic field. (c) . Temporal traces of THz emission from a multilayer spintronic device with in-plane magnetic anisotropy through a quartz waveplate.

was applied in the plane of the substrate to induce the anisotropy. Fig1. (b) shows the Stoner-Wohlfarth-like rotation of the magnetization measured with a vectorial magnetometer, compared with the amplitude of the THz signal components, obtained with a Time Domain Spectroscopy setup. Varying the magnetic field along the magnetic hard axis direction, we demonstrate a full 360° rotation of the THz polarization.

As an application of the coherent rotation control, we determined the birefringence properties of a quartz half-wave plate in the THz band. Quartz is a well-known optically anisotropic material that presents two light propagation axes, the ordinary and extraordinary axes. With the polarization control of our emitters, the difference of refractive index between the two axes can be easily evaluated in the THz range thanks to our Time Domain Spectroscopy setup.

The temporal shift between the observed peaks gives the index difference: $\Delta n = \Delta t \times \frac{c}{d}$, with Δt the temporal shift, c the speed of light and d the thickness of the quartz crystal. With a $\Delta t = 480fs$, the resulting index difference obtained is $\Delta n = 0.048$ between ordinary and extraordinary axis, which is consistent with values found in literature [3].

The authors thank the RENATECH network as well as the EU funded s-nebula project 863155.

References:

- [1]. Kampfrath, T., et al. Nature Nanotechnology, 8(4), 256–260, 2013.
- [2]. Kong, D., et al., Advanced Optical Materials, 7(20), 2019.
- [3]. Sakai, K., Stumper, U., IEEE Transactions on Microwave Theory and Techniques, 42(6), 956–965, 1994.

Magneto-electric control of polarization in spintronic terahertz emitters

Nicolas Tiercelin¹, Geoffrey Lezier¹, Pierre Koleják^{1,2}, Jean-François Lampin¹, Yannick Dusch¹, Kamil Postava² and Mathias Vanwolleghem¹

¹ Univ. Lille, CNRS, Centrale Lille, Univ. Polytechnique Hauts-de-France, UMR 8520 - IEMN - Institut d'Electronique de Microélectronique et de Nanotechnologie, F-59000 Lille, France

² Technical University of Ostrava, Nanotechnology Centre and IT4Innovations, Ostrava - Poruba, Czech Republic
Corresponding author: nicolas.tiercelin@iemn.fr

Polarization control of THz light is of paramount interest for the numerous applications offered in this frequency range. Recent developments in THz spintronic emitters allow for a very efficient broadband emission, and especially unique is their ability of THz polarization switching through magnetization control of the ferromagnetic layer[1]. So far, such a control has only been achieved using an external magnetic field. For the first time, we present here a scheme to achieve a voltage controlled coherent polarization rotation using a strain mediated magnetoelectric effect in spintronic emitters.

The considered emitter is a W(2nm)/ CoFe(0.5nm)/ TbCo₂(0.8nm)/ CoFe(0.5nm)/ Pt(2nm) stack deposited by RF sputtering in a LEYBOLD Z550 equipment on a 300 μm thick <011> cut PMN-PT ferroelectric relaxor. During the growth, a magnetic field was applied in the plane of the substrate in order to induce a well-defined uni-axial anisotropy that allows for a stoner-wohlfarth coherent rotation of the magnetization in the ferromagnetic layer. The CoFe/TbCo₂/CoFe tri-layer acts as an exchange-coupled multilayer and the 5d metals Pt and W provide the ISHE with opposite signs for their spin-Hall angles.

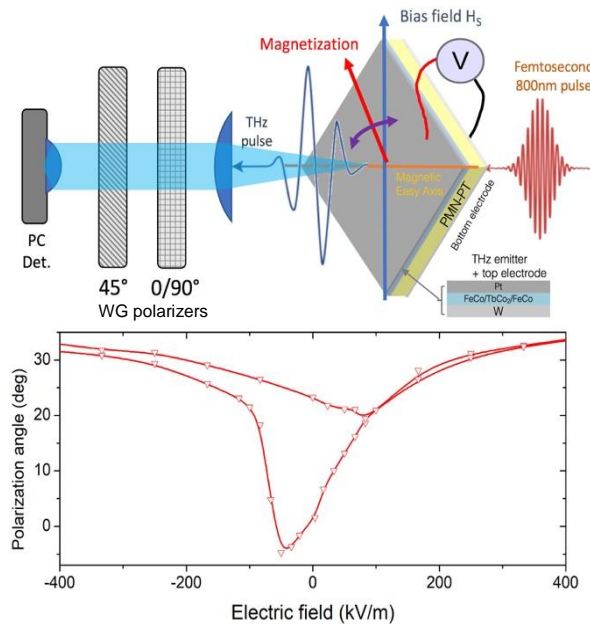


Fig. 1. Top: schematic representation of the magneto-electric spintronic emitter and characterization setup. Bottom: measured E-polarization angle with respect to the horizontal plane, as a function of the applied voltage on PMN-

The THz emission was characterized on a customized existing terahertz time-domain spectroscopy (TDS) setup. The ISHE-mediated terahertz emission is generated by pumping the sample with femtosecond pulses from a Ti:sapphire laser oscillator (80MHz repetition rate, center wavelength 800nm and 100fs pulse duration). The E-field of the emitted terahertz pulse is measured by sampling the response of a photo-conductive Auston switch that is probed by a split-off fraction of the femtosecond infrared pulse by a delay line. In order to measure the horizontal and vertical components of the E-field and deduce the polarization angle, two wire-grid polarizers were inserted in the THz path, as seen on figure 1. Setting the delay line to obtain the maximum signal amplitude, E-field components were measured while cycling the applied voltage on the PMN-PT substrate. A static magnetic bias is also applied to the

emitter. The deduced polarization angle is shown on figure 1, which clearly shows its controlled rotation over a span of nearly 40 degrees. Thanks to the magnetostrictive properties of the ferromagnetic tri-layer, and upon voltage application, the substrate generated stress induces a large change in magnetic anisotropy [2]. This in turn causes a coherent rotation of magnetization and thus of the emitted polarization. The hysteresis behavior reflects the hysteresis of the ferroelectric relaxor response.

References:

- [1] Seifert, T. et al. Nature Photonics, 10(7), 483–488 (2016) <https://doi.org/10.1038/nphoton.2016.91>
[2] N. Tiercelin et al. Appl. Phys. Lett., 99, 192507 (2011) - [doi: 10.1063/1.3660259](https://doi.org/10.1063/1.3660259)

Terahertz optomechanical resonators with bi-material structures

Jiawen Liu¹, Paolo Beoletto¹, Baptiste Chomet¹, Djamel Gacemi¹, Konstantinos Pantzas², Grégoire Beaudoin², Isabelle Sagnes², Yanko Todorov¹ and Carlo Sirtori¹

¹Laboratoire de Physique de l'Ecole normale supérieure, ENS, Université PSL, CNRS, Sorbonne Université, Université de Paris, 75005 Paris, France

²Centre de Nanosciences et de Nanotechnologies (C2N), CNRS—Université Paris-Sud/Paris-Saclay, Palaiseau 91120, France

Corresponding author: jiawen.liu@phys.ens.fr

In this presentation, we will report optomechanical resonators operating in the terahertz domain. We fabricated and characterized “dog-bone” and “split-ring” resonators with a suspended portion that acts as an oscillating beam converting THz signal into MHz frequency domain, which will then be probed by a read-out laser with high precision. Thanks to the bi-material structure (Au on top of GaAs), our resonators give very strong responses to the incident THz wave and thus can be employed as a sensitive THz detector operating at room temperature [1], or as a transducer between THz domains and other spectral domains [2].

In addition to terahertz detection or transduction, our system can also serve as a great platform for fundamental research when the mechanical oscillation is forced into a strong non-linear regime by a RF drive. As a preliminary result, we observed a spring-softening effect on our sample, indicating a negative nonlinear term in the Duffing equation. Combining the THz source with the RF drive, we can also demonstrate that, by changing the power or the modulation frequency of the THz wave, the nonlinear behavior of mechanical oscillators will be modified. In addition, mechanical combs can be synchronously generated on several oscillating modes at different frequencies. These effects will be further studied in our ongoing work.

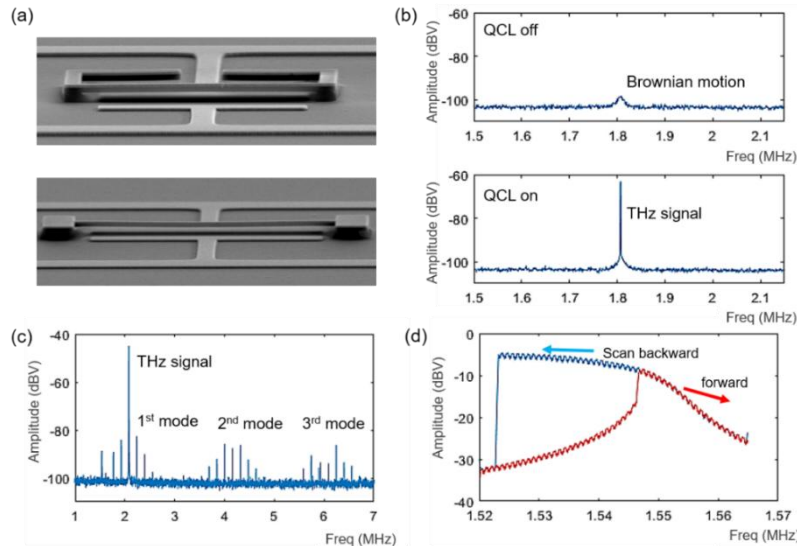


Fig. 1: (a) SEM images of split-ring (top) and dog-bone (bottom) resonator; (b) THz detection; (c) Comb generation in vacuum; (d) Duffing response in nonlinear regime.

References:

[1] C. Belacel et al. Nat Commun 8, 1578 (2017).

[2] A Calabrese et *al.* Nanophotonics 2019; 8(12): 2269–2277

Design and characterisation of Photoswitches for picosecond electric pulses generation at very low temperature

C. Bernerd¹, R. Pederiva¹, P. Artillan¹, C. Geffroy², G. Georgiou³, C. Bäuerle² and J.-F. Roux¹

¹Univ. Grenoble Alpes, Univ. Savoie Mont Blanc, CNRS, G INP, IMEP-LAHC, 73370 Le Bourget du Lac.

²Univ. Grenoble Alpes, CNRS, Institut Néel, 38042 Grenoble, France.

³Univ. of Glasgow, Glasgow, G12 8QQ, Scotland.

Corresponding author: jean-francois.roux@univ-smb.fr

The electrical ultrafast response of a Two-Dimensional Electron Gas (2DEG) system has been recently investigated at low temperature (4K) using a dedicated optoelectronic mesoscopic device [1]. Such an experiment typically takes benefit from THz technology as it relies on both the use of ultrafast photoswitches (PSW) integrated on-chip with the studied device and time equivalent sampling techniques. Therefore, such an approach should also allow for the time domain studies of 2DEG quantum electronic devices for which the coherence time of a single electron wavepacket (SEW) is typically in the 10-100 ps range [2]. However, the quantum regime of 2DEG requires that the device's temperature is kept below 0.1 K. So, it is mandatory to develop ultrafast PSW that present high optical to electrical conversion efficiency in order to generate, manipulate and detect SEW at a ps time scale without depositing too much optical power onto the chip. In this talk we will present the recent results that we obtained in the design, simulation and characterization of GaAs based ultrafast PSW dedicated to such quantum electronic experiments. First, we will focus on the different experimental set-ups used for the time domain characterization of PSW and their associated transmission lines (see Fig. 1). Then we will present different PSW designs addressing high optical to electrical conversion efficiency. These PSW involve plasmonic and electromagnetic resonances [3]. They are mainly inspired by 3D structures developed for photovoltaic solar cells [4].

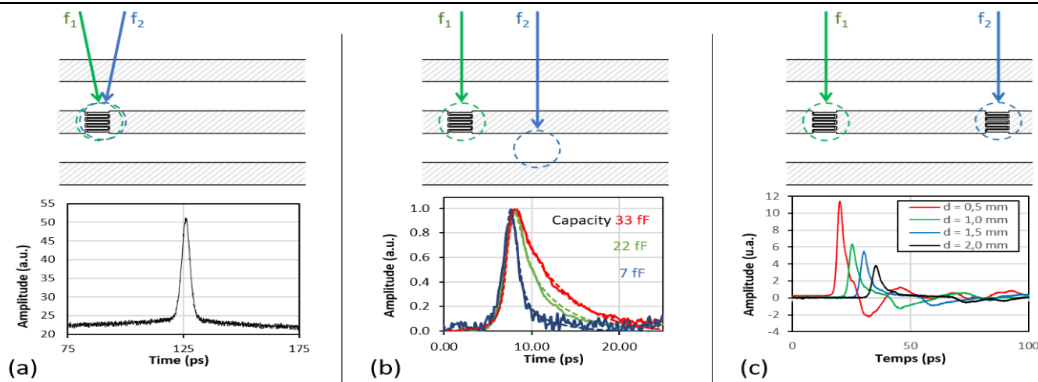


Fig. 1: Characterization of standard interdigitated 2D PSW and coplanar waveguides using different measurement configurations (a) autocorrelation, (b) sliding contact and (c) generation/detection.

Acknowledgments: We thank Pr. A. Wieck from Ruhr-Universität Bochum (Germany) for providing the 2DEG and LT-GaAGs layers. This work is supported by the ANR Projects, QTERA Grant ANR-2015-CE24-0007-02 and STEPforQubits, Grant ANR-2019-CE47-0005-01.

References:

- [1] J. Wu *et al.*, Sci. Rep. 5, 15420 (2015). DOI: 10.1038/srep15420
- [2] G. Roussely *et al.*, Nat Commun 9, 2811 (2018). DOI: 10.1038/s41467-018-05203-7
- [3] G. Georgiou *et al.*, ACS Photonics, 7, (6), 1444-1451 (2020). DOI: 10.1021/acsp Photonics.0c00044
- [4] J. Michallon *et al.*, Opt. Express 22, A1174-A1189 (2014). DOI : 10.1364/OE.22.0A1174

Photon-assisted tunneling in hBN encapsulated graphene quantum dot under coherent THz illumination

S. Messelot¹, E. Riccardi¹, S. Massabeau¹, M. Rosticher¹, K. Watanabe², T. Taniguchi², J. Tignon¹, S. Dhillon¹, S. Balibar¹, T. Kontos¹, J. Mangeney¹

1. Laboratoire de Physique de l'Ecole normale supérieure, ENS, Université PSL, CNRS, Sorbonne Université, Université Paris-Diderot, Sorbonne Paris Cité, Paris, France

2. National Institute for Materials Science, Tsukuba, Ibaraki, Japan

Corresponding author: juliette.mangeney@phys.ens.fr

Photon-assisted tunneling (PAT) is an attractive process for the study of light-matter interaction phenomena. In PAT, the electron tunneling through a quantum dot is enabled via the quantum absorption of an electromagnetic wave. Up to now, only a few works and a few quantum systems have demonstrated PAT under THz illumination [1-3]. Graphene quantum dots (GQD) of typical size ~ 100 nm size have great potential for PAT under THz illumination as their energy level splitting to quantum electron confinement falls in the THz range [4], and room temperature bolometric detection of THz radiation have been demonstrated in GQD-based devices [5].

Here, we investigate the quantum response of hBN encapsulated GQD to coherent THz illumination and demonstrate photon-assisted tunneling. We fabricate a single electron transistor made of a hBN encapsulated GQD of 120 nm diameter connected to source and drain electrodes by two narrow constrictions (40 nm) and surrounded by three lateral gates: G_1 , used to control the quantum dot chemical potential, and G_2 and G_3 , used to set the two constrictions as tunneling barriers (Fig 1(a)). The device is placed in a dilution $^4\text{He}-^3\text{He}$ cryostat at 40 mK with optical access, enabling its illumination with coherent THz radiation from a GaAs Schottky diodes source. Without illumination, the electronic transport in the GQD is in the Coulomb blockade regime as illustrated in Fig 2(b)-left: at low SD bias voltage, an electron can tunnel through the GQD only if a GQD energy level is available between energy levels of source and drain. As a consequence, the tunneling current through the quantum dot exhibits the Coulomb peaks pattern as the GQD chemical potential is swept using the G_1 gate voltage (black curve, Fig 1(c)).

As we switch the THz coherent illumination on, a new transition can be enabled through the absorption of a THz photon: Fig 2 (b)-right illustrates a possible mechanism for this photon-assisted tunneling, and shows the GQD chemical potential shift associated to this new transition is given by the energy of the absorbed photon. Our experimental measurement exhibits an additional satellite current peak whose gate voltage shift increases as the THz illumination frequency increases (highlighted by dashed line Fig 1 (c)). This frequency dependence matching the dependence expected from PAT indicates we observe PAT in our experiments. This demonstration of light matter interaction between coherent THz radiation and discrete electronic levels in GQD opens up very interesting perspectives for both fundamental studies and the development of quantum THz devices.

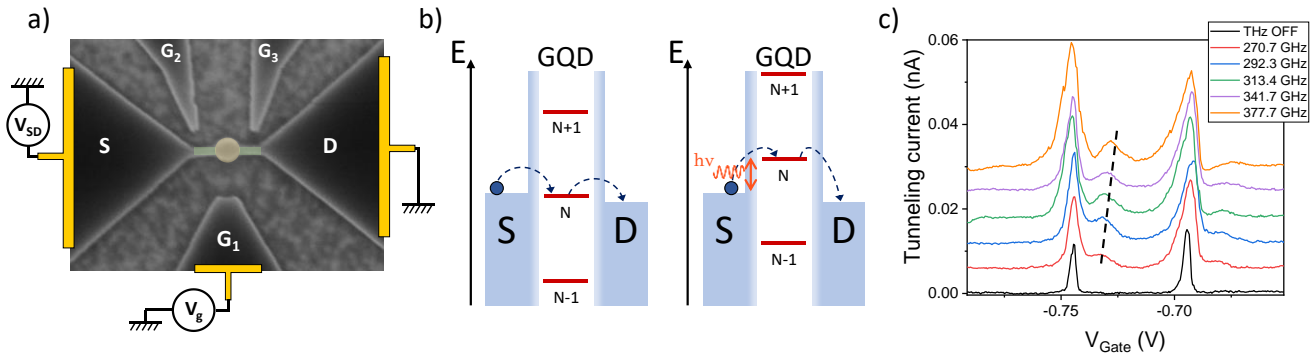


Fig. 1: **a)** SEM picture of the hBN encapsulated GQD including schematics of the connected electrodes and bias/gate voltages. **b)** Energy diagram illustrating the tunneling process of an electron from source to drain electrodes through the GQD. Left: tunneling without illumination. Right: tunneling mediated by the absorption of a THz photon. **c)** Experimental measurement of the tunneling current under illumination through the GQD presented Fig (a) for increasing THz excitation frequency, offsetted for clarity.

References:

- [1] S. Zeuner et al., “Photon-assisted tunneling in GaAs/AlGaAs superlattices up to room temperature”, *Appl. Phys. Lett.* 69, 2689 (1996)
- [2] N. Orihashi et al., “One THz harmonic oscillation of resonant tunneling diodes”, *Appl. Phys. Lett.* 87, 233501 (2005)
- [3] M. Rinzan, et al., “Carbon Nanotube Quantum Dots As Highly Sensitive Terahertz-Cooled Spectrometers.”, *Nano Letters*, 12, pp. 3097-3100, (2012)
- [4] Stampfer et al., “Tunable Coulomb blockade in nanostructured graphene”, *Appl. Phys. Lett.* 92, 012102 (2008)
- [5] A. El Fatimy et al., “Epitaxial graphene quantum dots for high-performance terahertz bolometers”, *Nature Nanotechnology*, 11, pp. 335–338, 2016.

ON-CHIP TWO-OCTAVES SUPERCONTINUUM GENERATION IN MID-IR SIGE WAVEGUIDES

M. Montesinos-Ballester¹, N. Koompai¹, C. Lafforgue¹, J. Frigerio², A. Ballabio²,
X. Le Roux¹, E. Herth¹, J R. Coudevylle¹, D. Bouville¹, A. Barzaghi², C. Alonso-
Ramos¹, L. Vivien¹, G. Isella², D. Marris-Morini¹

¹Centre de Nanosciences et de Nanotechnologies, Université Paris-Saclay, CNRS, 91120
Palaiseau, France

²L-NESS, Dipartimento di Fisica, Politecnico di Milano, Polo di Como, Via Anzani 42, 22100
Como, Italy

Corresponding author: natnicha.koompai@u-psud.fr

Mid infrared spectroscopy is a widely used technique to perform molecular sensing, as most of the molecules have their fundamental vibrational and rotational resonance in this spectrum range. Each molecule absorbs light at the specific wavelength and produces a unique absorption pattern in the spectra that makes it possible to identify the targeted molecules. In this context, we present the experimental study of on chip supercontinuum generation in the mid-infrared range, Thanks to a Ge-rich graded-index platform, second-order dispersion engineering and low propagation losses are achieved. A broad spectrum is obtained from 3 to 13 μm wavelength (a spectral band of more than 2500 cm^{-1}) for a pump wavelength at $8.5\text{ }\mu\text{m}$, in a 5.5 mm long waveguide. Moreover, both results from numerical and experimental outcome are in agreement. Therefore, this work leads to the development of many mid-infrared wideband applications.

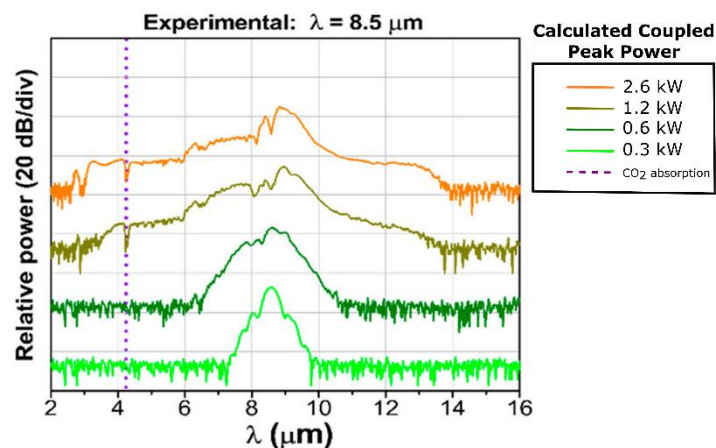


Fig. 1: Generation of supercontinuum: experimental output in a 5.5 mm long waveguide for different values of optimal peak power, for input pump at $8.5\text{ }\mu\text{m}$ wavelength.

References:

[Type the document title]

[1] M. Montesinos-Ballester et al., On-Chip Mid-Infrared Supercontinuum Generation from 3 to 13 μm Wavelength. *ACS Photonics*. 7(12): 3423-3429, 2020.

Sub wavelength resonator coupled to colloidal nanocrystal array for short wave infrared sensing with near unity absorption

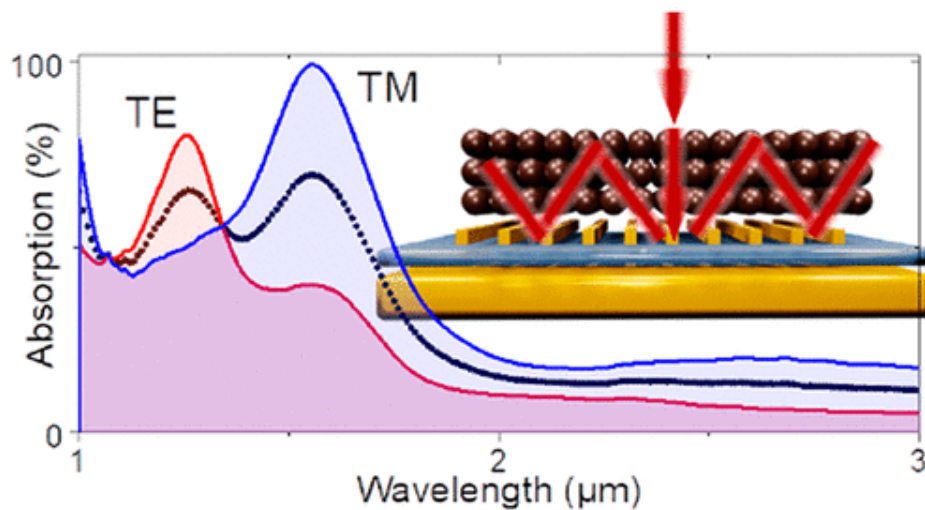
Audrey Chu^{1,2}, Charlie Gréboval¹, Yoann Prado¹, Tung Huu Dang¹, Adrien Khalili¹, Gregory Vincent², Emmanuel Lhuillier¹

¹ Sorbonne Université, CNRS, Institut des NanoSciences de Paris, INSP, F-75005 Paris, France

² ONERA -The French Aerospace Lab, 6, chemin de la Vauve aux Granges, BP 80100, F-91123 Palaiseau, France

Corresponding author: lhuillier@insp.upmc.fr

Nanocrystal synthesis has reached a high level of maturity enabling fine shape and size control over a broad range of materials. Using material such as HgTe, it is possible to tune the absorption spectrum all over the infrared range from 800 nm and up to the THz¹. Beyond basic light absorption, nanocrystal photoconductive properties are now coupled to read out circuit and, focal plane array operating in the SWIR range have been obtained.² However, the polycrystalline nature of nanocrystal films leads to hopping conduction generally associated with short carrier diffusion length. The latter is typically at least 10 times shorter than the absorption depth and consequently nanocrystal film have a weak absorption: 10 % for a 200 nm thick film at 2.5 μm . To overcome this tradeoff between absorption and charge conduction, we introduce into the device a guided mode resonator (GMR), in order to generate a mode propagating along the substrate enabling multi passes of the light.³ GMR device is designed to achieve 100 % of the TM light absorption. We also take care about electromagnetic field localization to avoid thermal losses. In our device, around 70 % of the absorption is localized within the nanocrystal film. I will finally show that this approach is versatile and can also be applied to phototransistor⁴ and photodiode⁵ geometry.



References:

- (1) Gréboval, C. et al. E. Mercury Chalcogenide Quantum Dots: Material Perspective for Device Integration. *Chem. Rev.* 2021, 121, 3627–3700.
- (2) Chu, A. et al. HgTe Nanocrystals for SWIR Detection and Their Integration up to the Focal Plane Array. *ACS Appl. Mater. Interfaces* 2019, 11, 33116–33123.
- (3) Chu, A. et al. Near Unity Absorption in Nanocrystal Based Short Wave Infrared Photodetectors Using Guided Mode Resonators. *ACS Photonics* 2019, 6, 2553–2561.
- (4) Gréboval, C. et al. Ferroelectric Gating of Narrow Band-Gap Nanocrystal Arrays with Enhanced Light–Matter Coupling. *ACS Photonics* 2021, 8, 259–268.
- (5) Rastogi, P. et al. Complex Optical Index of HgTe Nanocrystal Infrared Thin Films and Its Use for Short Wave Infrared Photodiode Design. *Advanced Optical Materials*, 2002066.